Distortion and Disintegration of Injected Liquid Streams
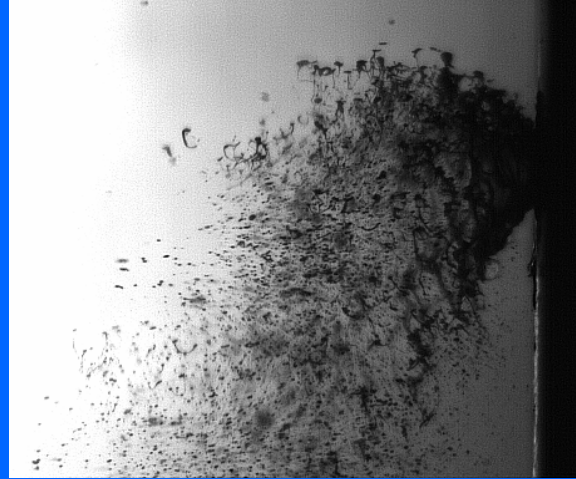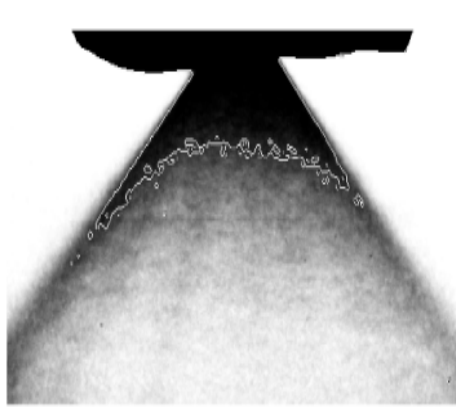
William A. Sirignano

University of California, Irvine
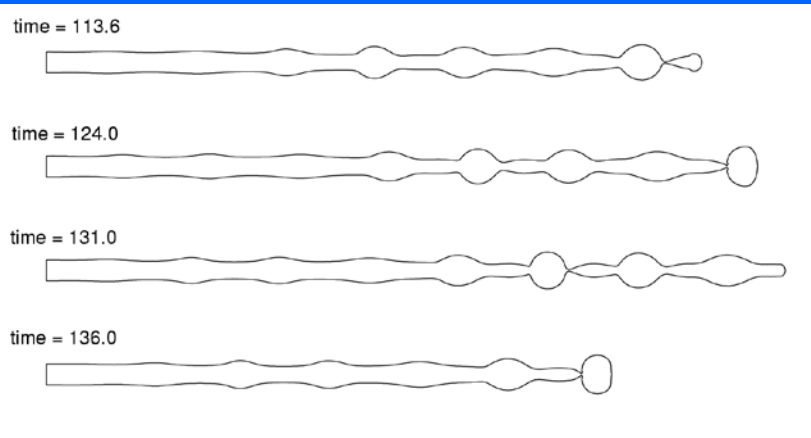
Round jets with and without aerodynamic effects
Planar jets with and without aerodynamic effects
Annular and "conical" jets with and without swirl
Cavitation and bubble growth, distortion, and collapse
Start-up and shut-down transients

Practice: Swirling annular sheet into stagnant gas or cross flow

time = 113.6

time = 124.0

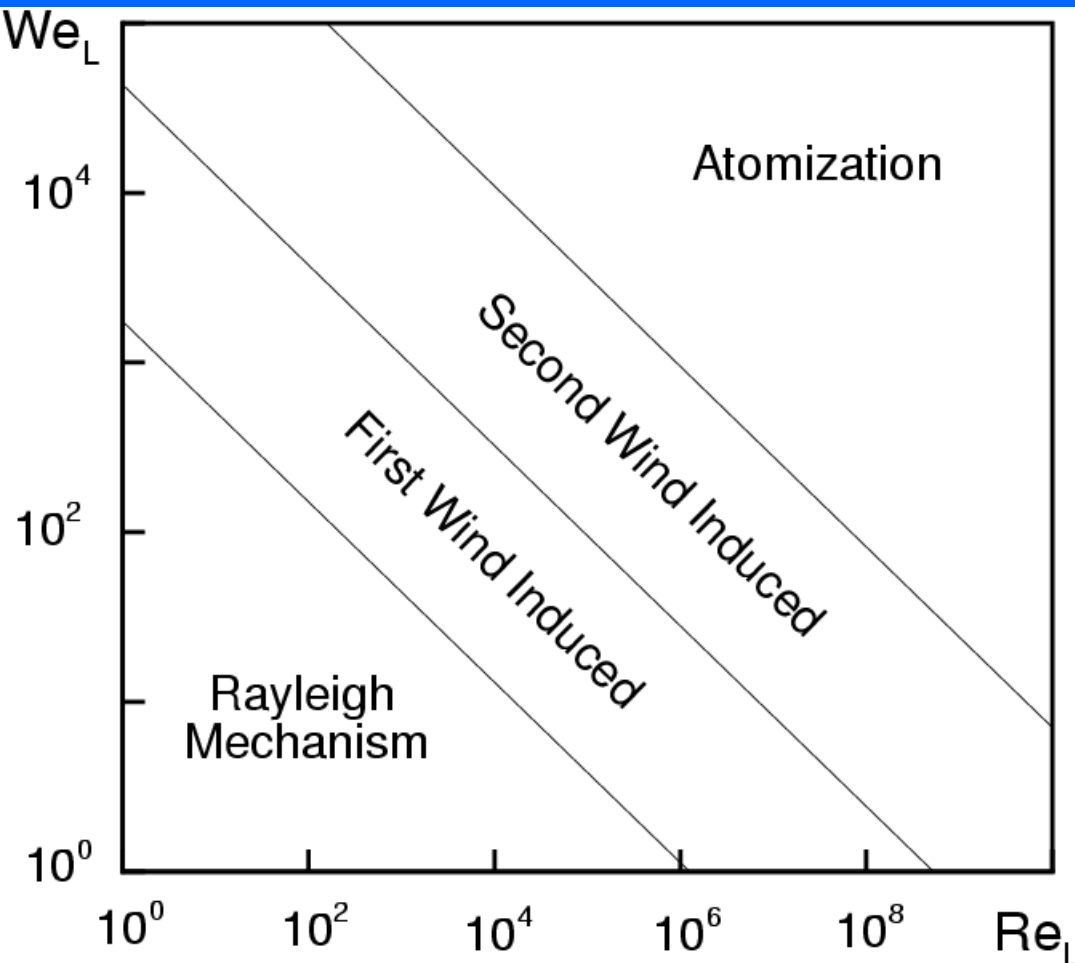time = 131.0

time = 136.0

Classical Rayleigh break up of cylindrical column of liquid.
Mean velocity of jet is irrelevant.

y

z

x
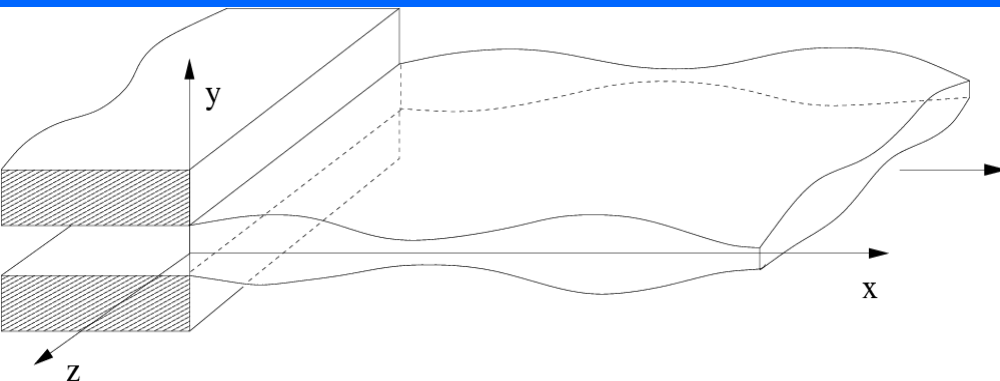
Model of perturbed thin planar liquid sheet (free film).
Theory has been extended to annular and "conical" sheets

Breakup of Cylindrical Jet

Atomization is a practical regime of high Weber and Reynolds numbers. Most of the energy for break-up and creation of new surface energy comes from kinetic energies of gas and liquid. Wide droplet size distribution.

For **Rayleigh break-up**, Weber and Reynolds numbers and gas kinetic energy are irrelevant; each can be zero. Behavior is symmetric, monodisperse.

Transitional Regimes:
Axisymmetry disappears in first wind-induced regime
with smaller droplets appearing in second wind-induced regime.

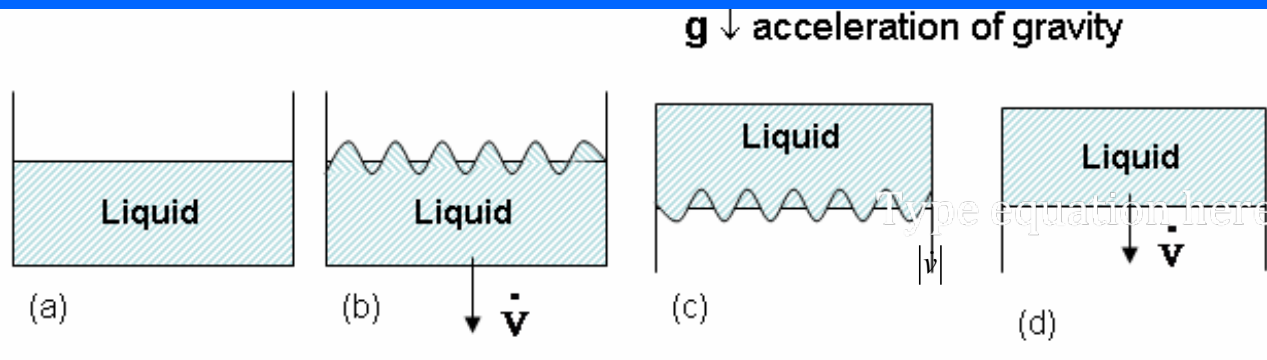# Kelvin-Helmholtz (KH) / Capillary Instabilities
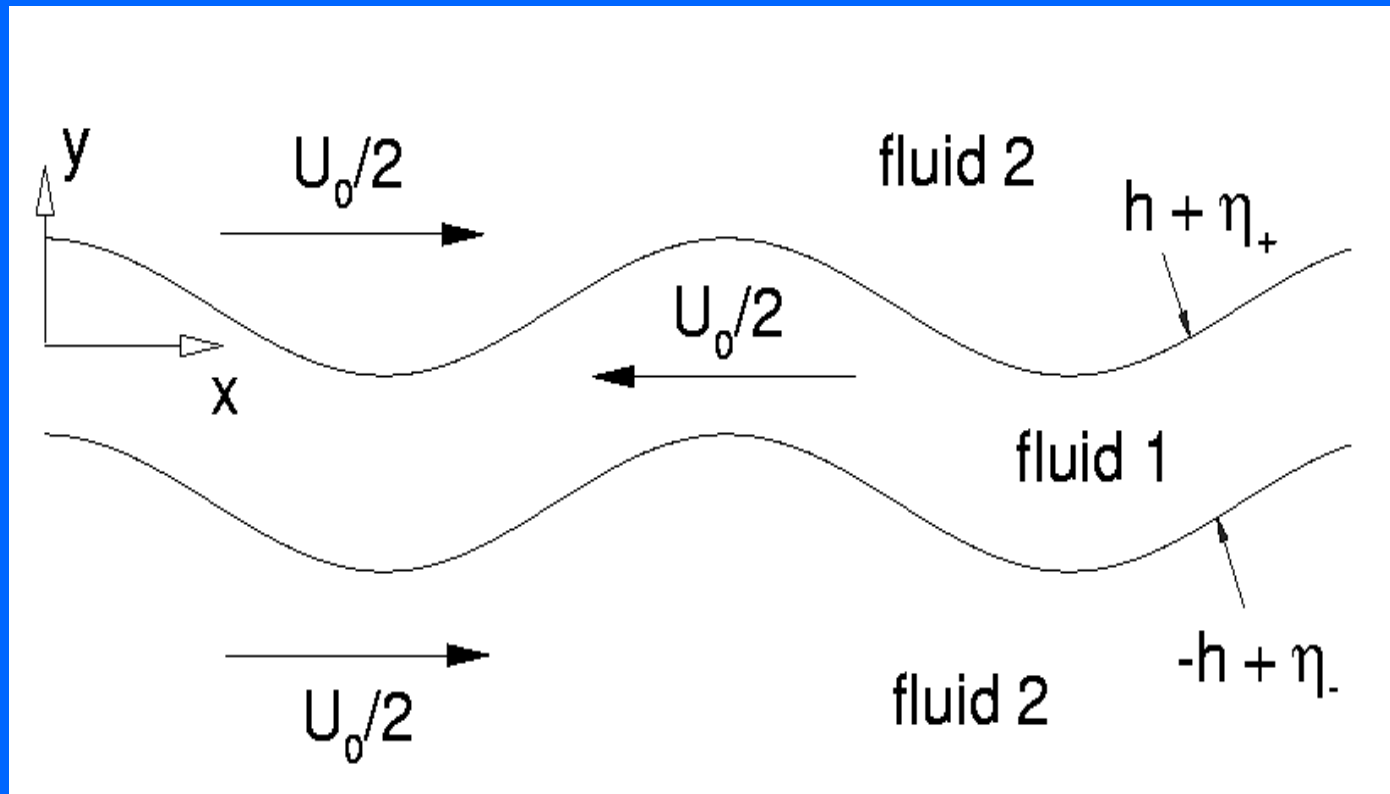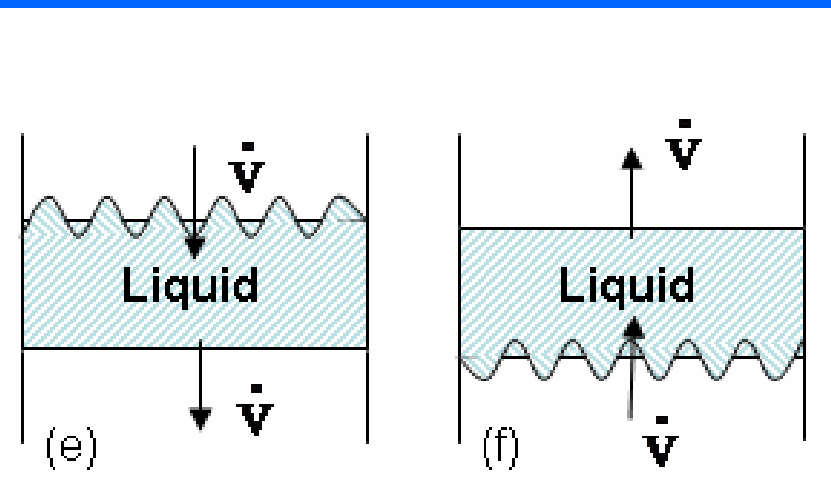

Parallel incompressible gas streams;

$\rho = \rho_2/\rho_1$, $We_1 = \rho_1 U_0 \lambda / \sigma$, $We_2 = \rho_1 U_0 h / \sigma$, λ / h

Rayleigh–Taylor (RT) Instability
Acceleration normal to liquid surface
|dv/dt| > g

Home experiment with a glass of water. *Warning: dress properly.*

Open cylinder on two ends:
(e) accelerating mass of free liquid, breakup on back side;
(f) decelerating mass of free liquid, breakup on forward side.

BASIC FORCES AND NONDIMENSIONAL GROUPS

Gravity force	-	$\rho_l L^3 g$
Inertia	-	$\rho_l L^2 V_l^2$
Surface tension force	-	σL
Viscous force	-	$\mu_l L V_l$

Reynolds number	Re	$= \rho_l L V_l / \mu_l$	Density ratio	-	ρ_l / ρ_g
Weber number	We	$= \rho_l L V_l^2 / \sigma$	Viscosity ratio	-	μ_l / μ_g
Froude number	Fr	$= V_l^2 / gL$	Velocity ratio	-	V_l / V_g
Ohnesorge number	Oh	$= \mu_l / (\rho_l \sigma L)^{0.5}$			

Instability criteria for oil-air interface

Legend:
- All effects
- Viscosity missing
- Gravity missing
- Surface tension missing
- Inertia missing

x-axis: wave length(m)
y-axis: real part of growth rate (1/sec), $\times 10^8$
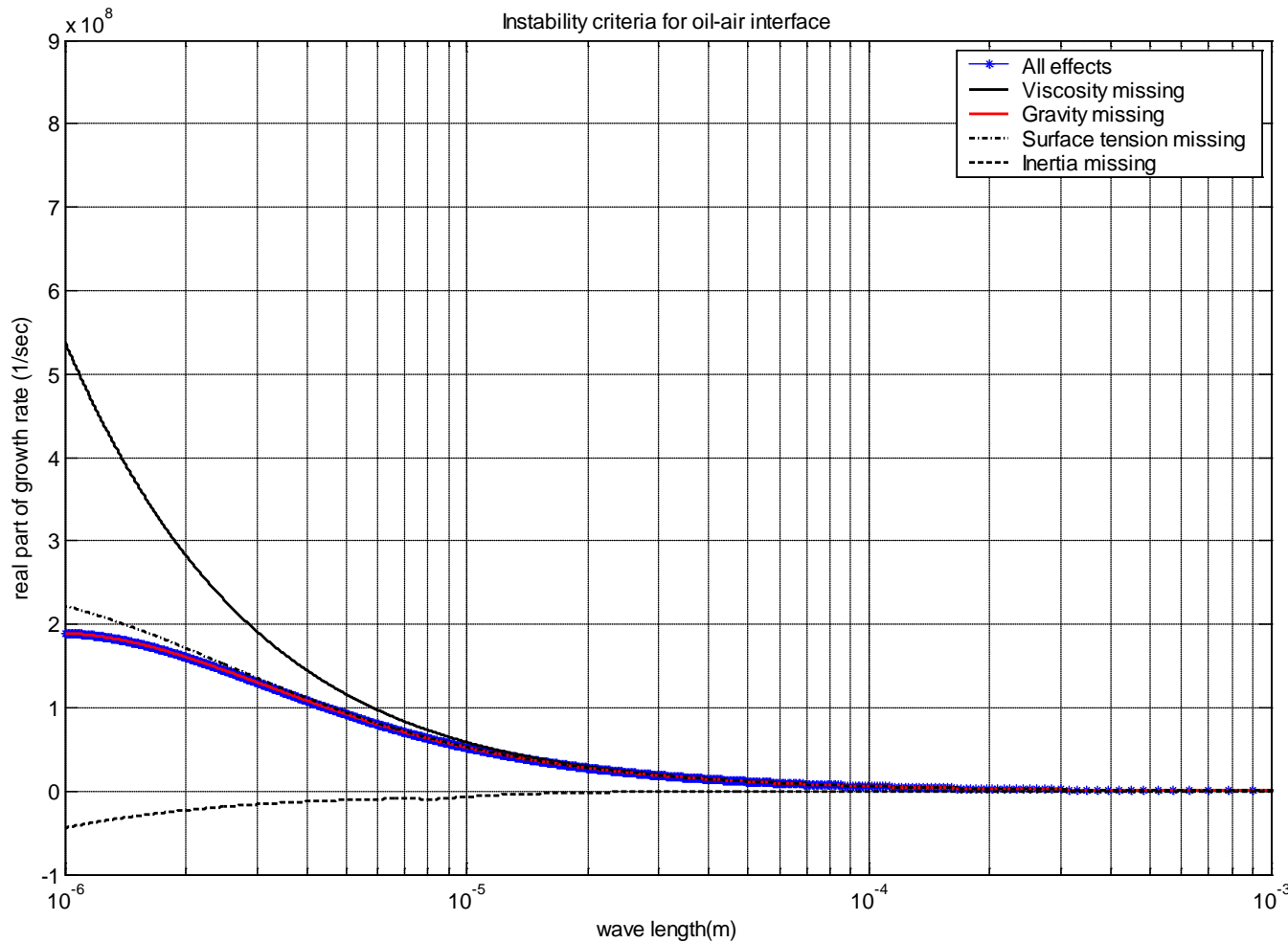
γ = surface tension coefficient

k = wave number

g = gravitational acceleration
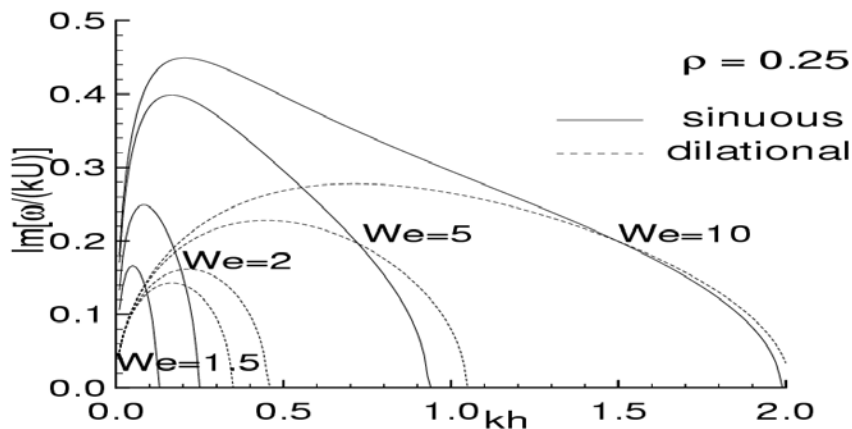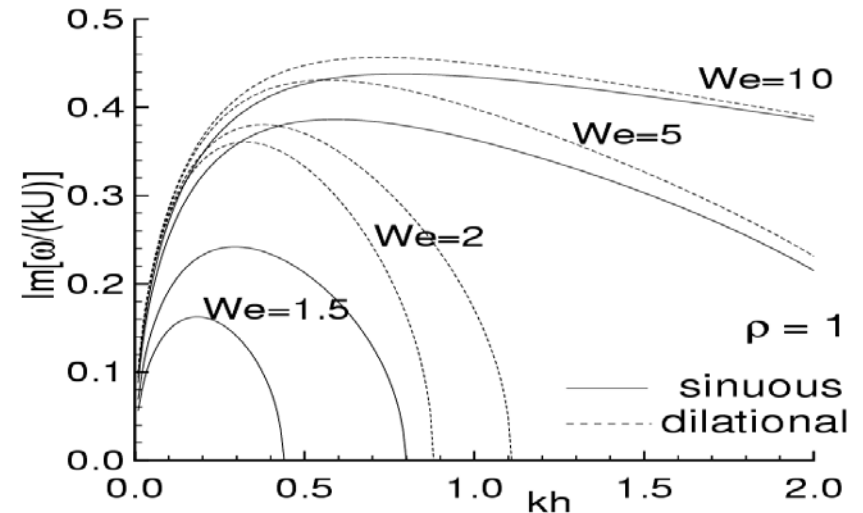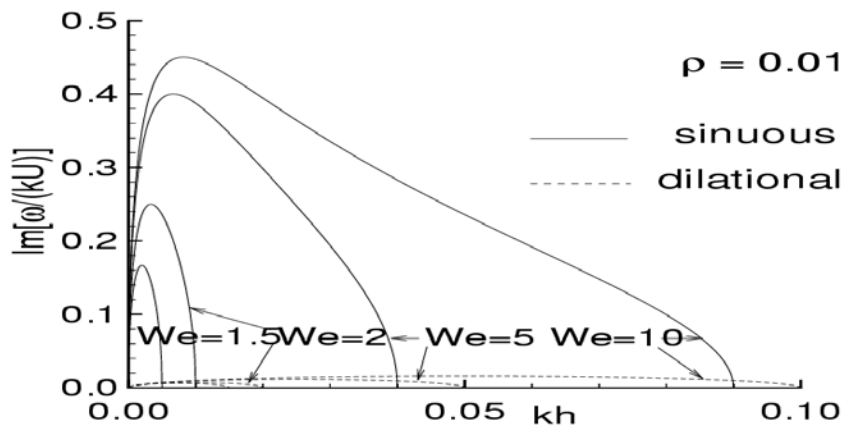
ρ_a, U_a = air density and velocity

ρ_l, U_l = liquid density and velocity

$$\sigma_R = -\frac{k^2(\mu_a + \mu_l)}{(\rho_a + \rho_l)} \pm \left[\frac{\rho_a \rho_l k^2 (U_a - U_l)^2}{(\rho_a + \rho_l)^2} - \frac{(\rho_l - \rho_a)gk + \gamma k^3}{(\rho_a + \rho_l)} + \frac{k^4(\mu_a + \mu_l)^2}{(\rho_a + \rho_l)^2} \right]^{1/2}$$

$$\sigma_I = -\frac{k(\rho_a U_a + \rho_l U_l)}{(\rho_a + \rho_l)}$$
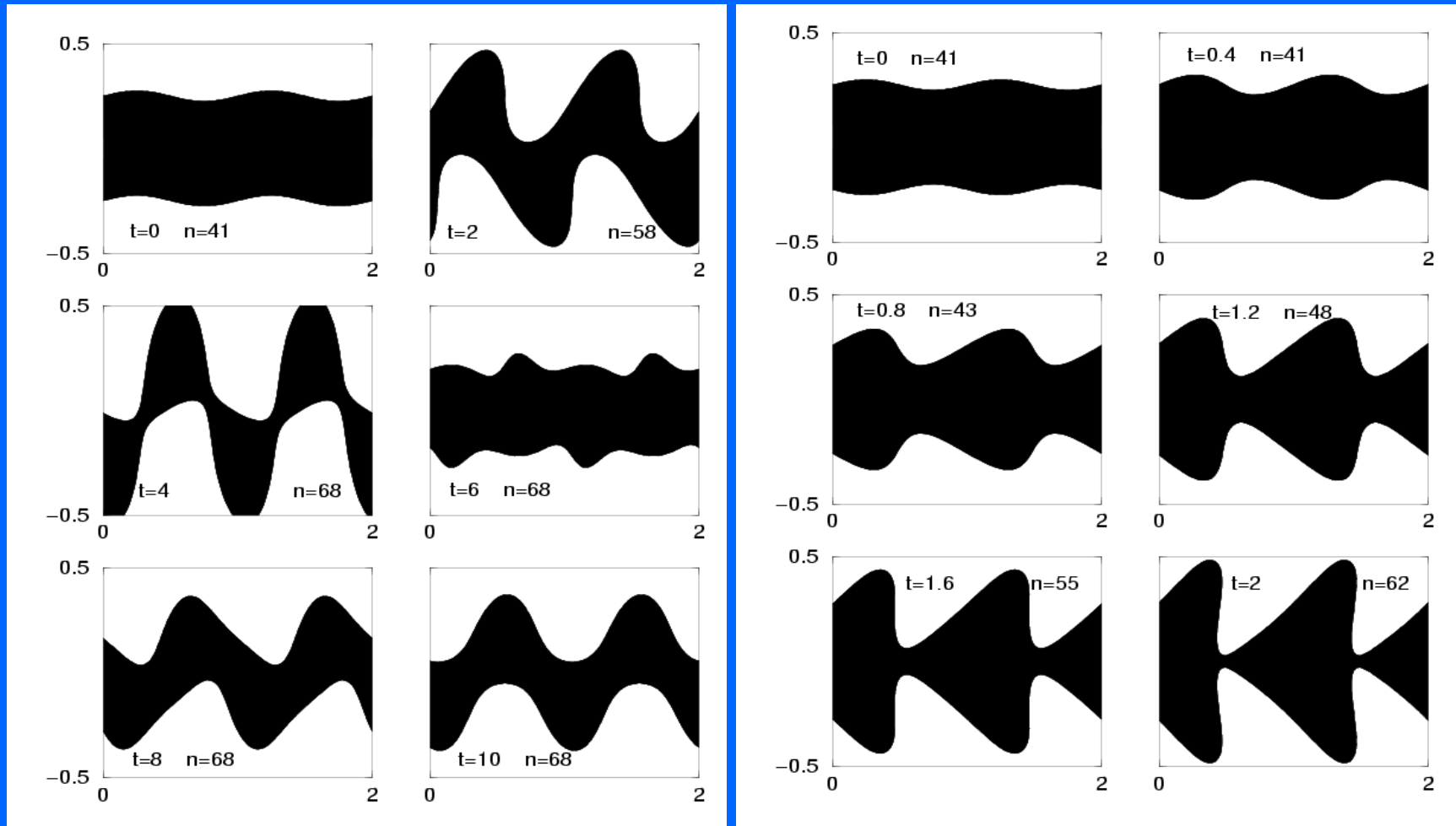
Linear Theory of KH Instability for Planar Sheet Spatially Periodic – Temporal Instability

Sinuous (antisymmetric) mode is more unstable at low pressures as observed experimentally but dilational (symmetric) mode is more unstable at high pressures.

Nonlinear Planar KH / Capillary Instability - Vortex Dynamics

Interfaces are treated as vortex sheets with capillary stress; inviscid potential flow exists on each side; discontinuities in velocity and density across interface. Temporal, spatially periodic instability.

Planar Sheets – Reduced Dimension Approach
Air Inertia Effects

Liquid-phase equations for velocity and film thickness.

dilational mode.

$$\frac{\partial \tilde{y}}{\partial t} + \frac{\partial (\overline{u}\tilde{y})}{\partial x} = 0$$

$$\frac{\partial \overline{u}}{\partial t} + \overline{u}\frac{\partial \overline{u}}{\partial x} = \frac{\sigma}{2\rho_l}\left[f\frac{\partial^3 \tilde{y}}{\partial x^3} + \frac{\partial f}{\partial x}\frac{\partial^2 \tilde{y}}{\partial x^2}\right] - \underbrace{\frac{1}{\rho_l}\frac{\partial p_g}{\partial x}}$$

$$f = \left[1 + \frac{1}{4}(\partial\tilde{y}/\partial x)^2\right]^{-3/2}$$

Two equations combine to give a dispersive wave equation. (Two more equations for v and centerline position for sinuous wave.)

Gas-phase:

(potential flow)

$$\nabla^2 \phi_g = 0$$

$$\frac{\partial \phi_g}{\partial t} + \frac{1}{2}(\nabla\phi_g)^2 = -(p_g - p_{g,0})$$

Coupling: pressure difference across interface equals capillary pressure.
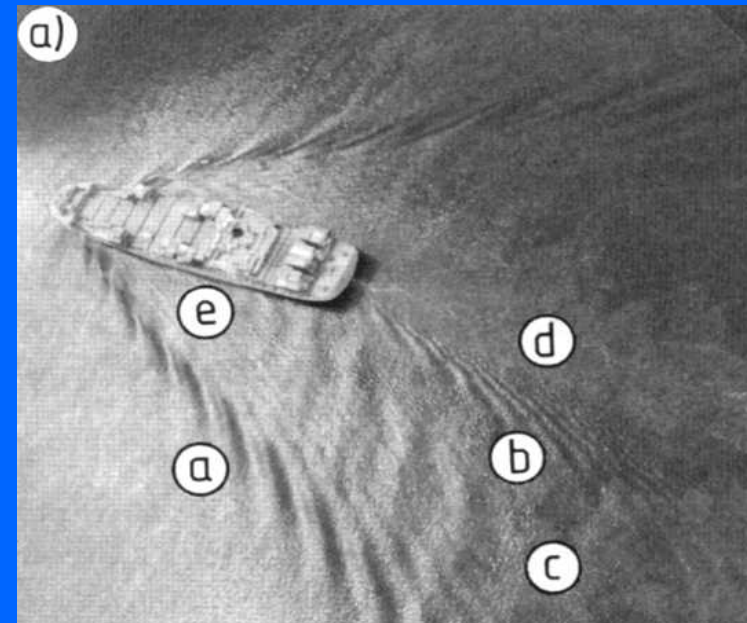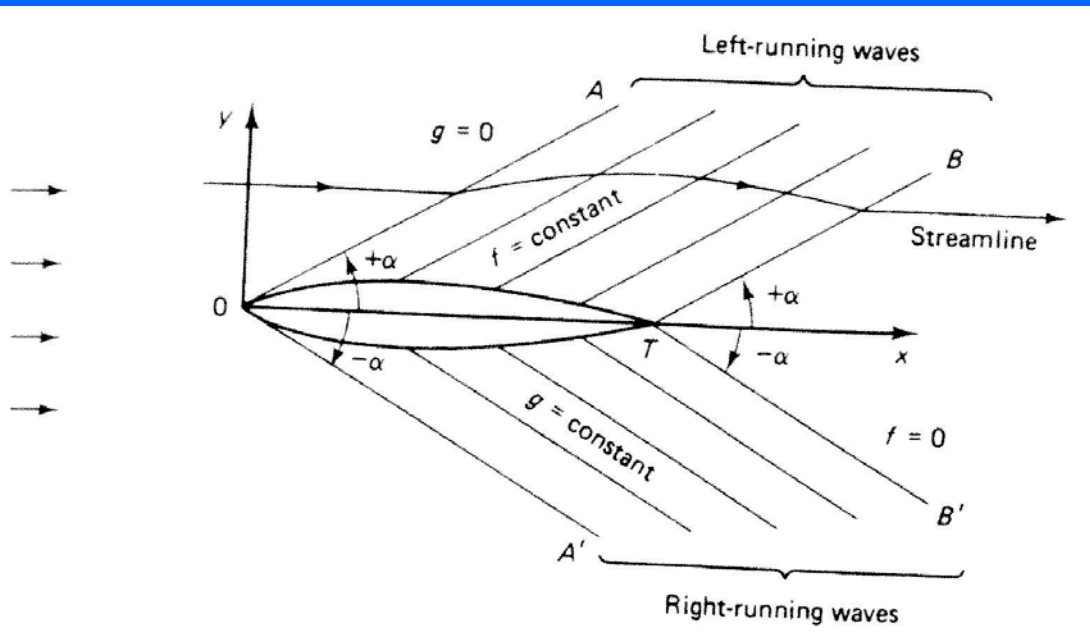
GROUP VELOCITY
Conservation of the number of wave peaks or troughs as the wave travels means that

$$\frac{\partial k_i}{\partial t} + \frac{\partial \omega}{\partial x_i} = 0 \quad ; \quad or \quad \frac{\partial k_i}{\partial t} + U_j \frac{\partial k_i}{\partial x_j} = 0 \; ;$$

$$where \quad \omega = \omega(k_1, k_2, k_3) \; ; \; U_j = \frac{\partial \omega}{\partial k_j}$$

U_j is the group velocity.
Information and energy propagate at the group velocity

Four solutions for linear dispersive spatially developing capillary dilational wave; four complex wave numbers k as functions of frequency or time period. Injection into a semi-infinite domain.

$$\frac{\partial^2 \tilde{y}}{\partial t^2} + \frac{\partial^4 \tilde{y}}{\partial \xi^4} = 0 \; ; \; \xi = x - u\,t$$

$$\tilde{y} = c\,e^{\,i(\omega t - k\,x)}$$

Only two solutions propagate information downstream (positive group velocity): k_2 and k_3.
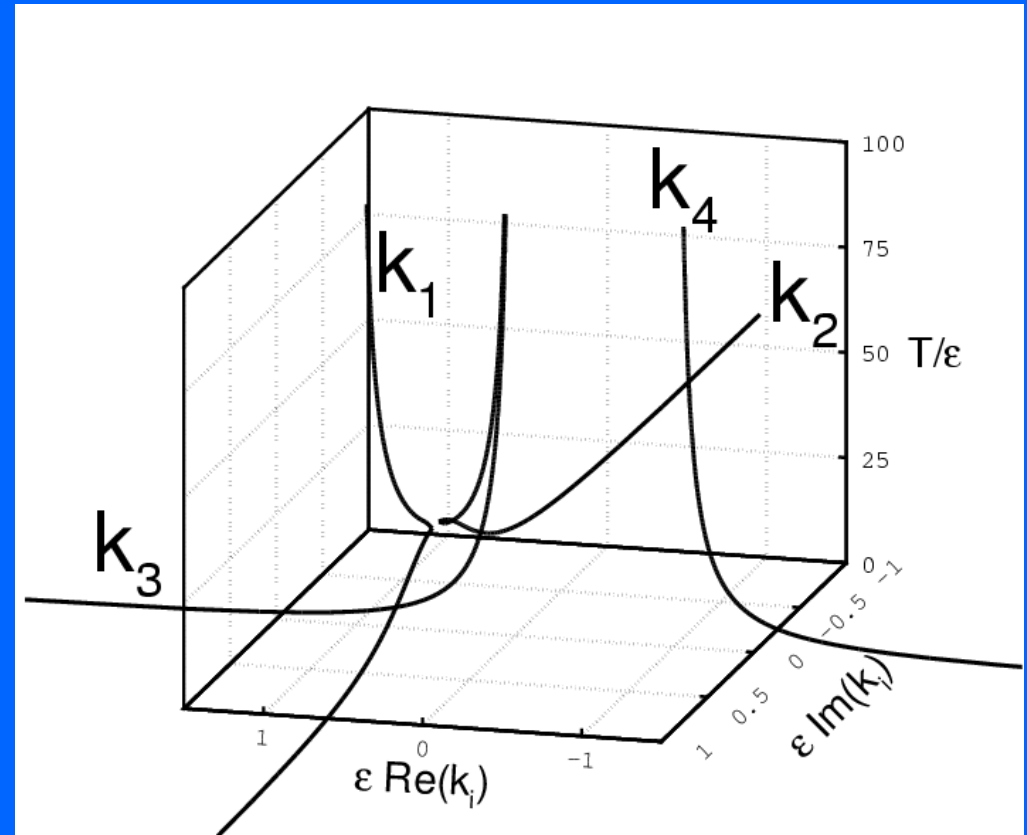
The other two propagate information upstream and are zeroed by quiescent boundary conditions at infinity . A negative imaginary part of k_2 implies spatial decay in flow direction Only can have stream breaking by beat phenomenon.

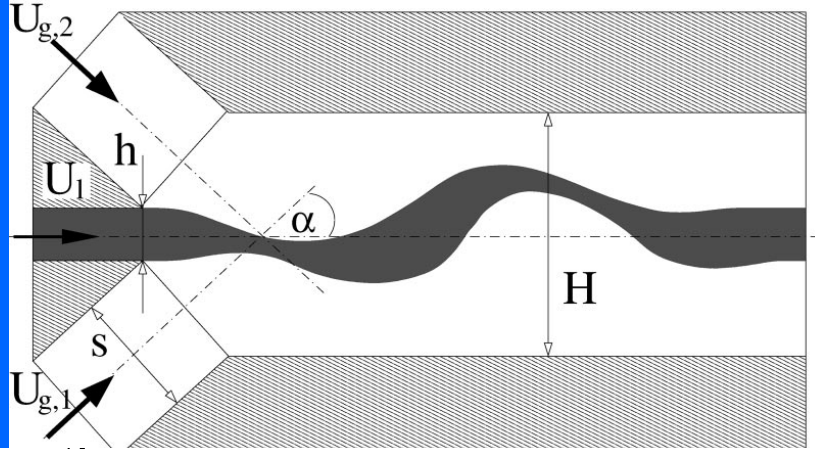Nonlinear effects cause substantial deviation from sinusoidal behavior.

Pinch-off can occur.
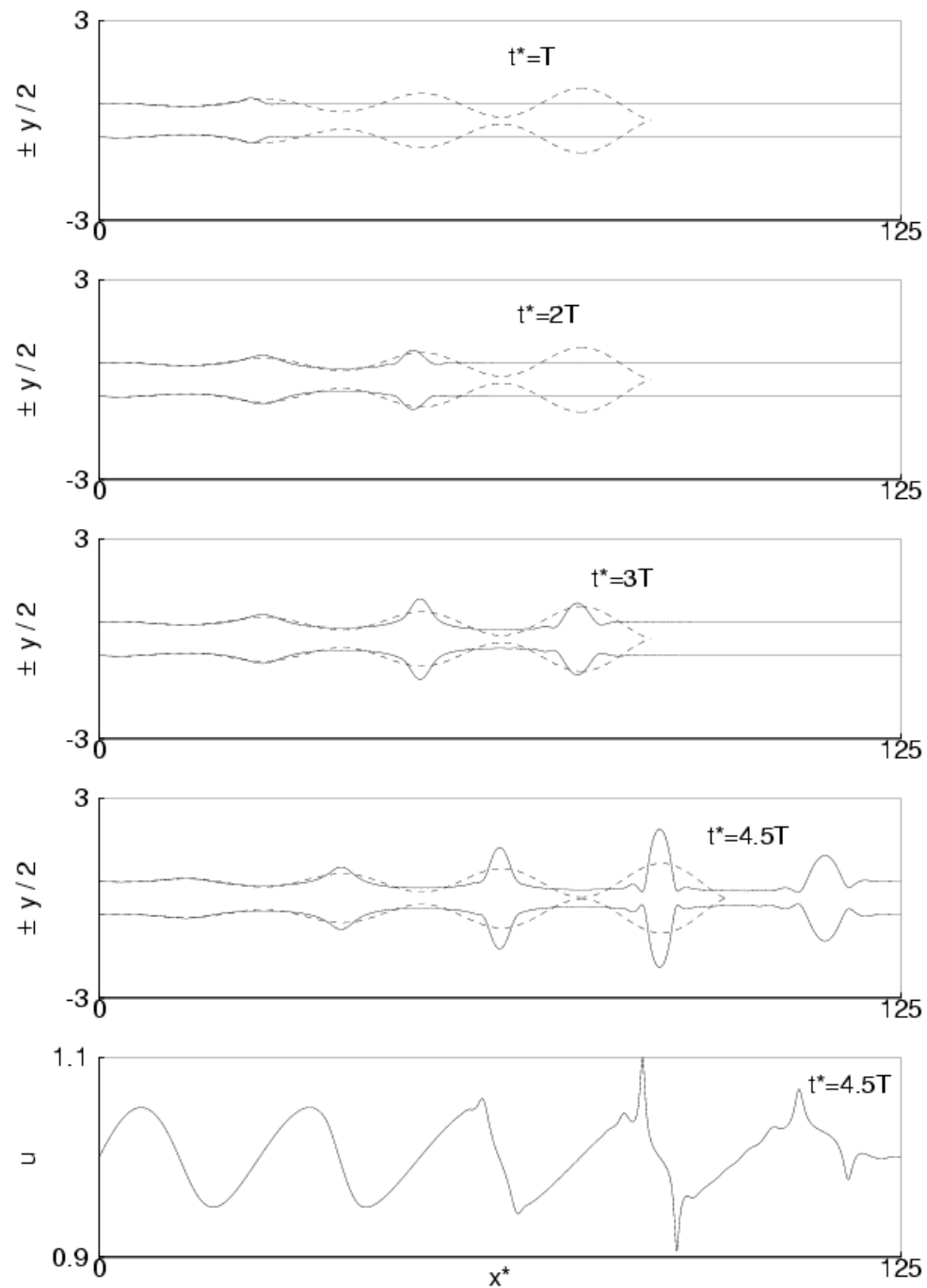
Antisymmetric (sinuous) nondispersive waves can also appear. For linear wave, centerline position is governed by

$$\frac{\partial^2 \overline{y}}{\partial t^2} = \frac{\partial^2 \overline{y}}{\partial \xi^2}$$

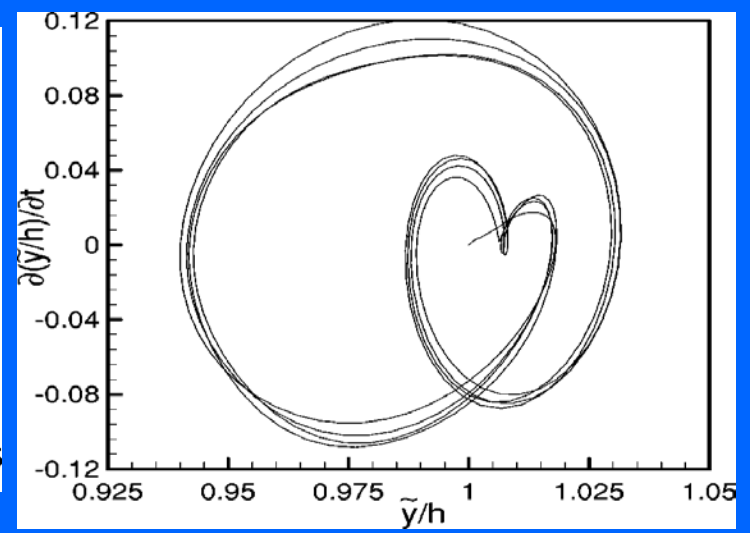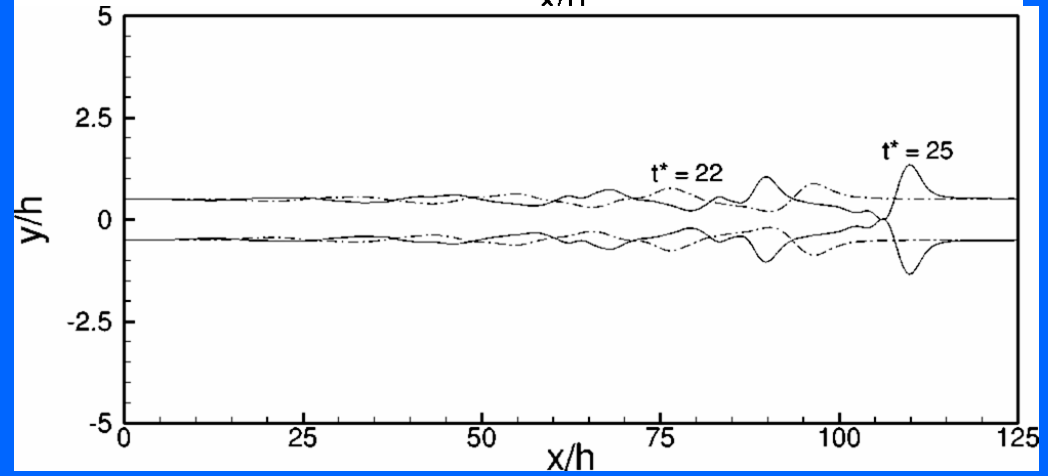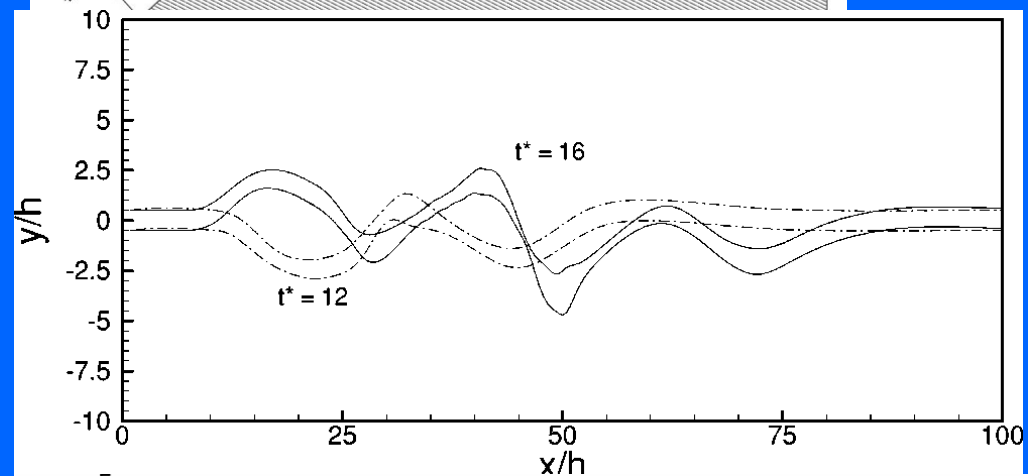Only two solutions with no growth or decay. Nonlinear effects superimpose a dilational effect.
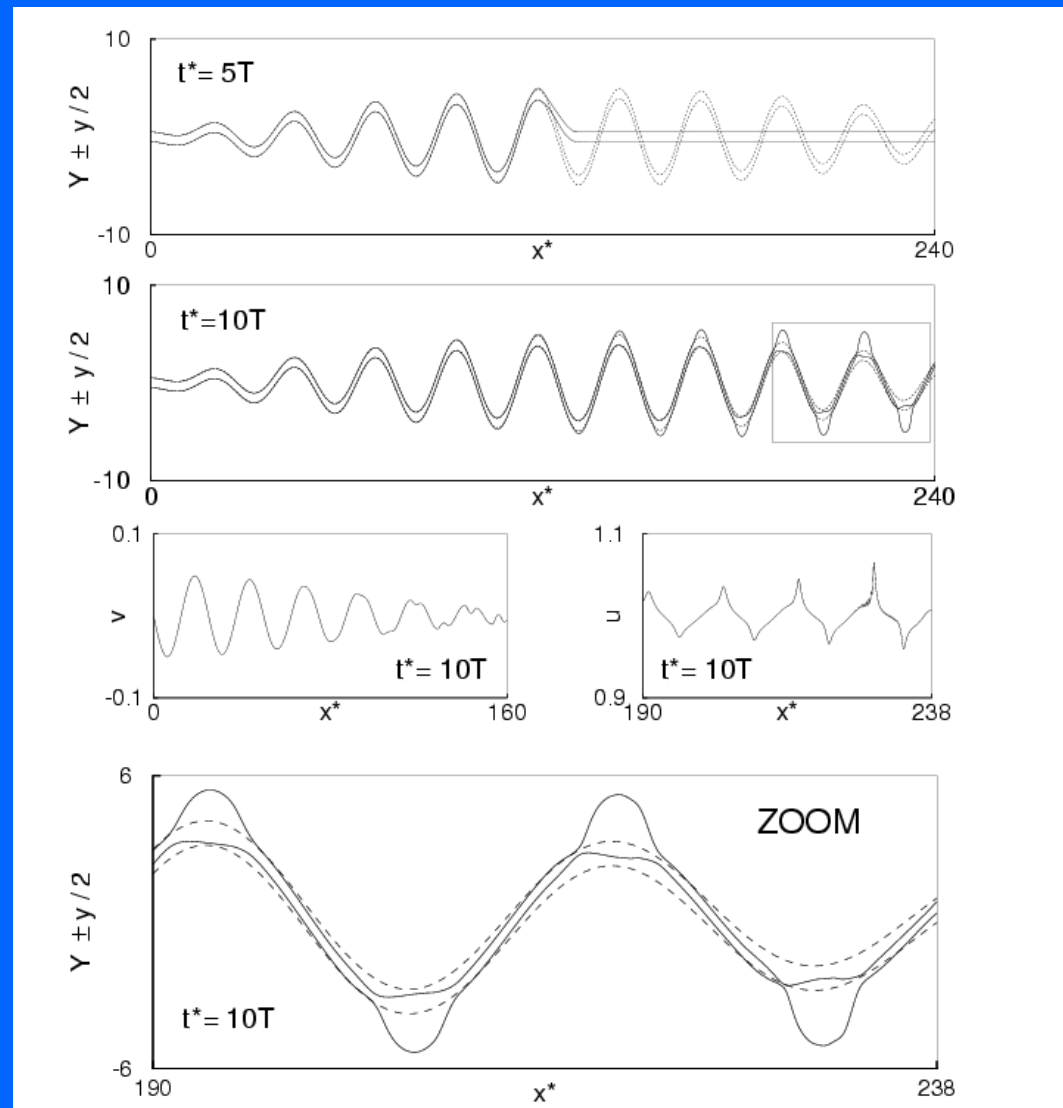
Pulsed gas injection can excite instability quickly.

In-phase pulses generate symmetric instability.

Out-of-phase pulses generate antisymmetric instability.
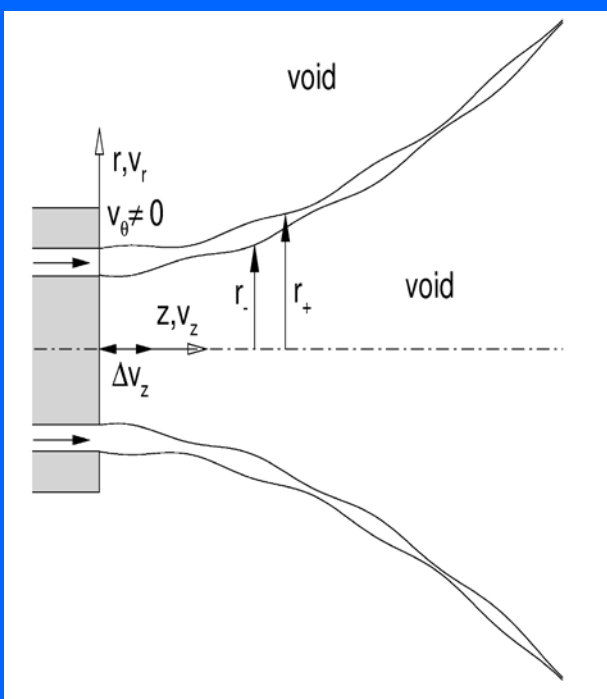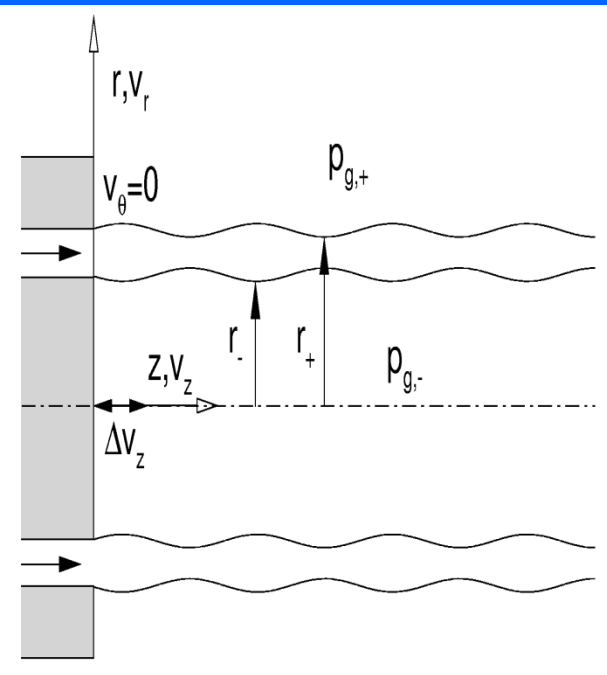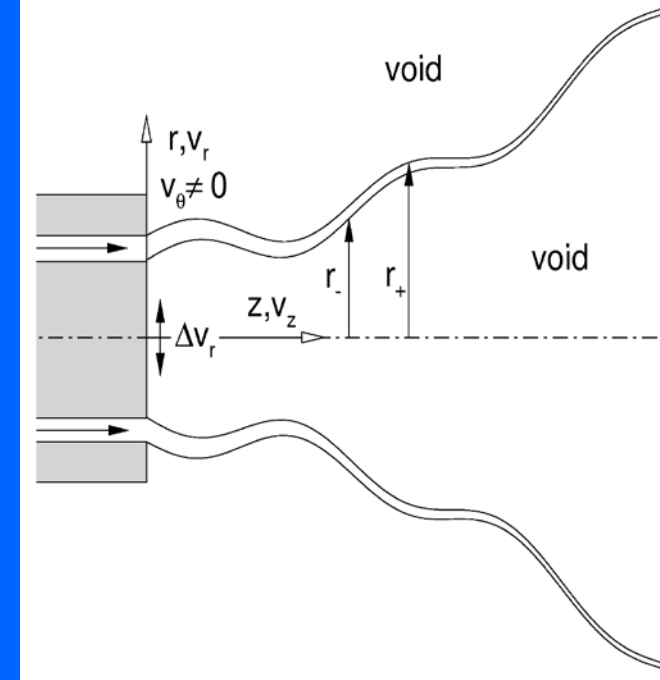
Chaotic motion can result.

ANNULAR MODES

← Dilational, "symmetric" or "sausage" mode
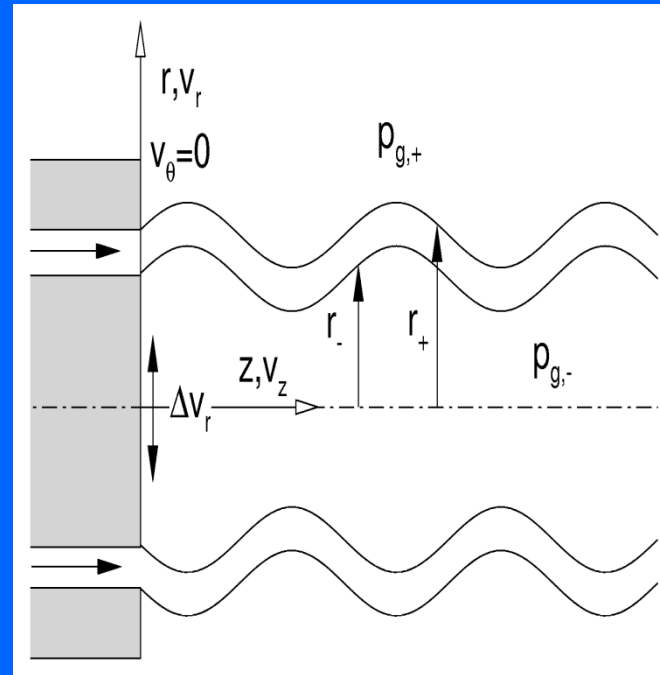
Sinuous or → "antisymmetric" mode

"CONICAL" MODES

Annular modes can be stabilized by swirl or by pressurization of the interior. Without such a mechanism, capillary force would collapse the liquid film. Swirl is more practical.

Again, four dilational modes and two sinuous modes are found in spatially developing case. Now, the sinuous waves are dispersive as well.
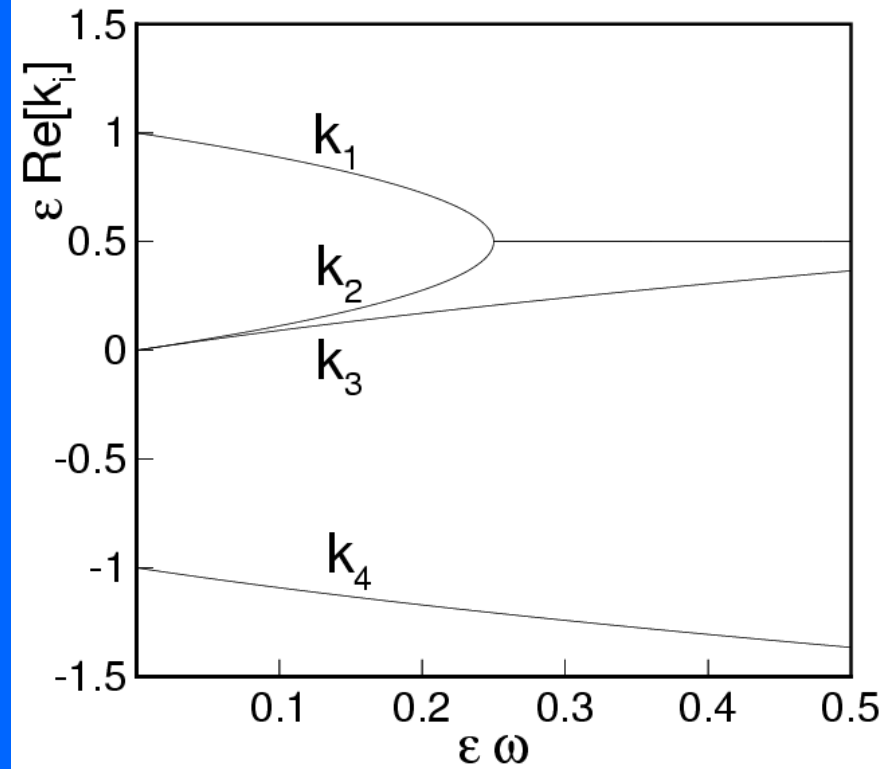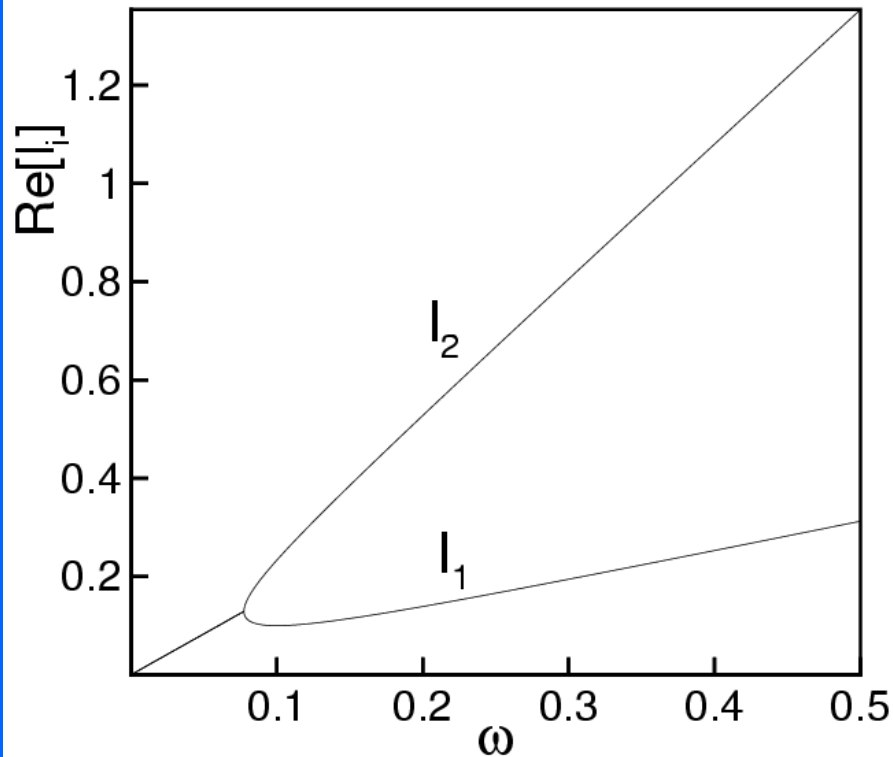
Examples of behavior for dilational and sinuos modes in annular configuration.

Annular radius is an important parameter which introduces a new characteristic length and results in an additional capillary force.
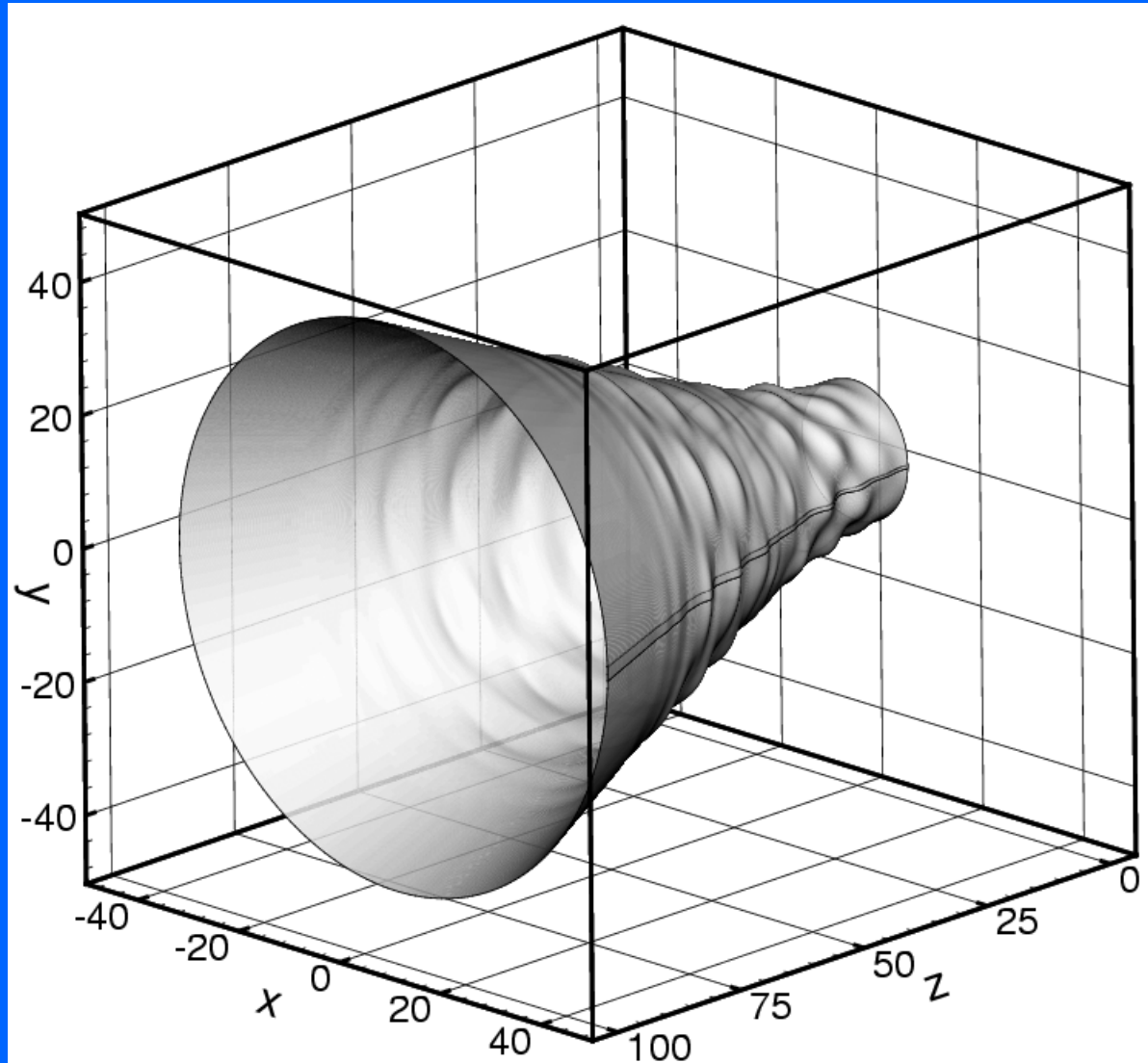
Still, qualitative similarities with the planar case remain.
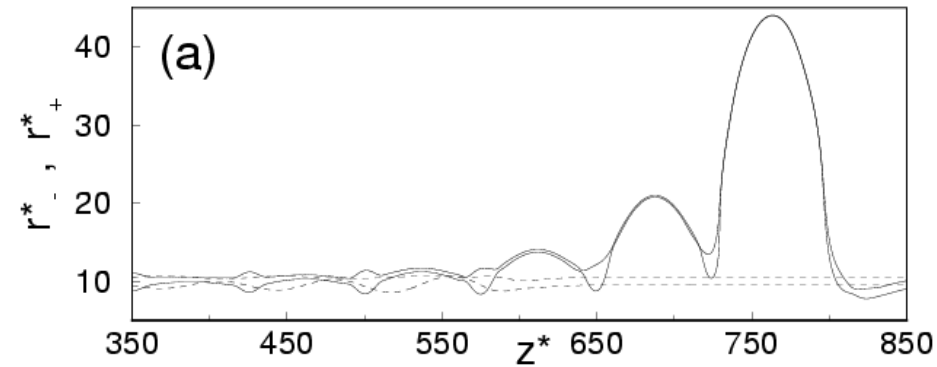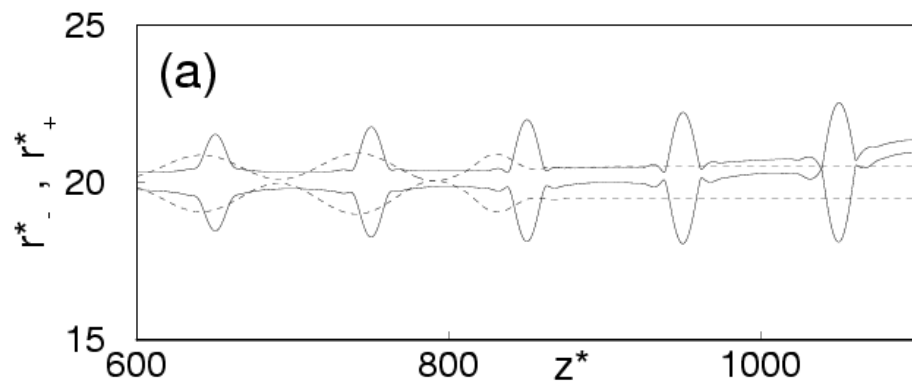
Conical "three-dimensional" calculation with swirl and Sinuous modulation at exit of annular nozzle.
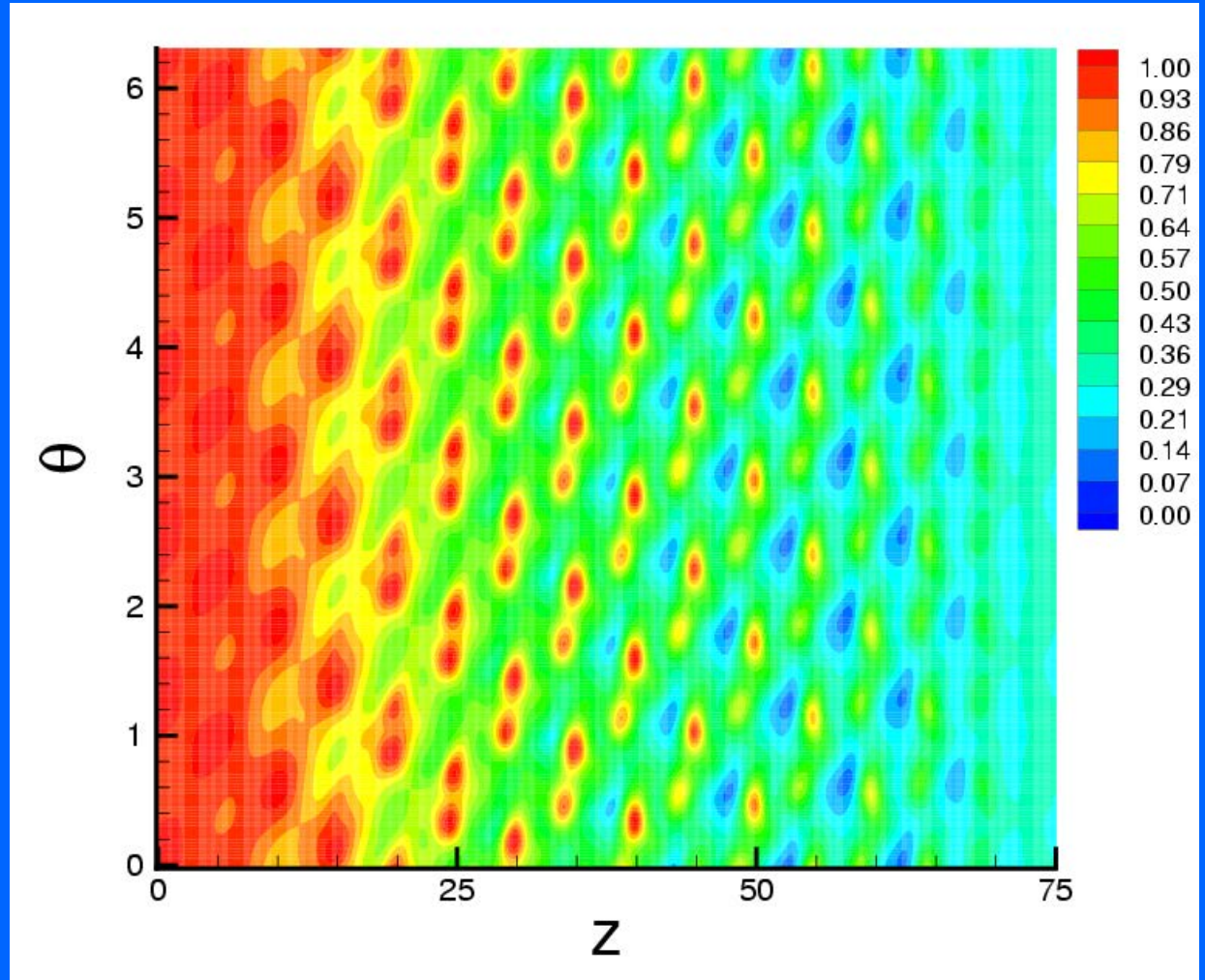
Outer surface is shown at a particular instant.

Thin spots result and lead to local tearing of the sheet.

Local film thickness is shown in contour plot for a particular instant. Flow is from left to right. Theta indicates azimuthal position. The blue spots

The blue spots Develop with downstream flow and indicate positions for likely tearing of the liquid film.

Cavitation in the Injector Orifice

- Better jet atomization is observed with cavitation inside the nozzle. (Tamaki et al. 1998, 2001, Hiroyasu 2000)

- Cavitation has been observed at pressures too high to explain by pressure criterion. (Winer and Bair, 1987; Joseph 1998, 2001)

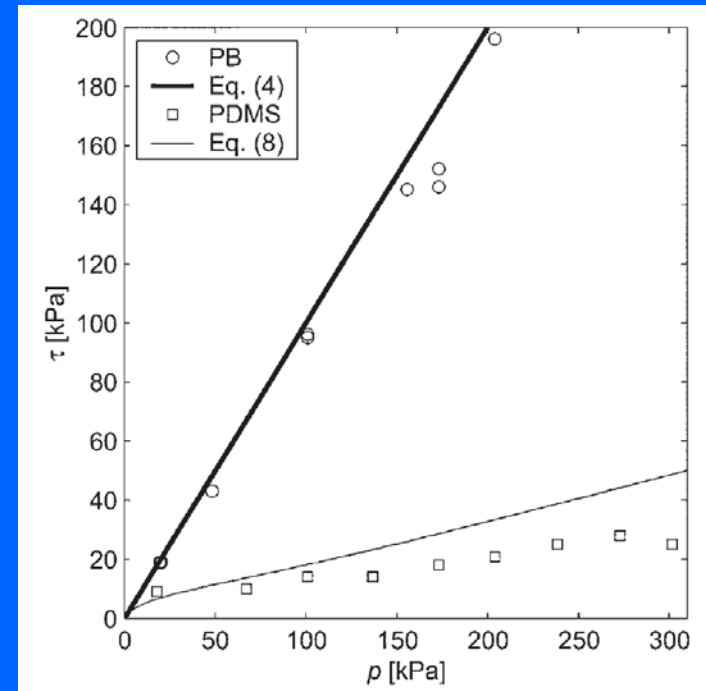- Disturbances caused by collapse of cavitation bubbles lead to instability of jet.
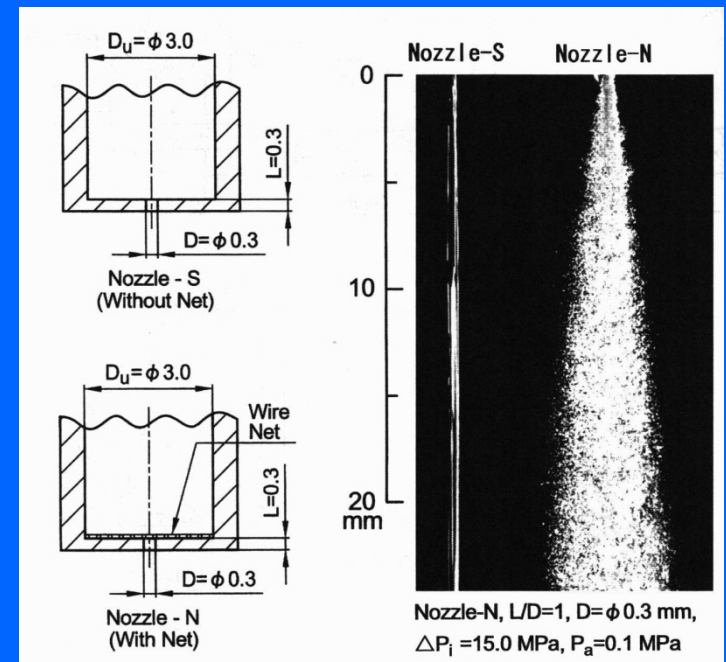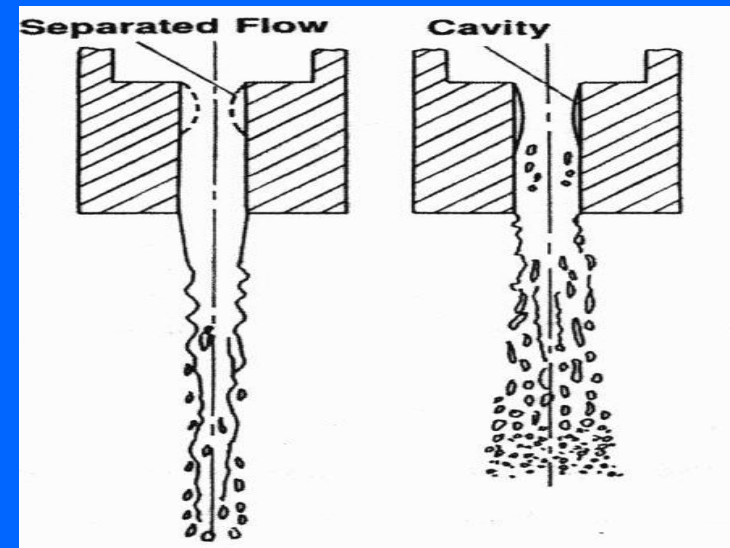
Effect of cavitation (from Hiroyasu 2001)

Stress-Induced Cavitation

- Experiment by Kottke, Bair and Winer (2005)
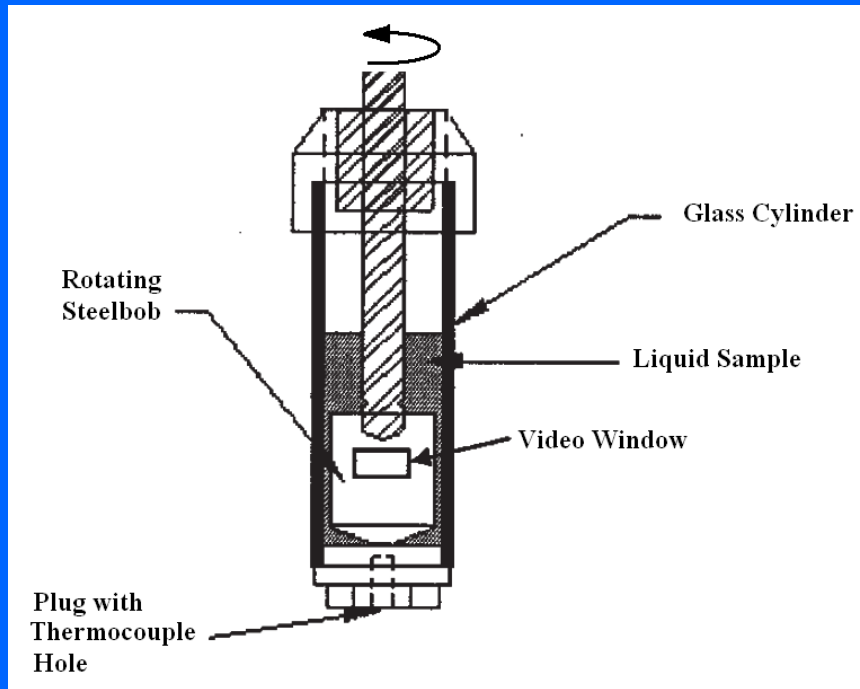
Variable pressure Couette viscometer

Shear stress at beginning of cavitation as a function of pressure for polybutene (Newtonian) and polydimethylsiloxane (non-Newtonian).

Cavitation criteria

- Critical pressure (stress): p_c
- Two criteria for cavitation:
  - Pressure criterion: $p < p_c$
  - Total-stress criterion proposed by Winer and Bair (1987) and independently by Joseph (2001):

  $$T_{11} > -p_c$$

  (Maximum principal stress) $\mathbf{T} = \mu \left[(\nabla \mathbf{u}) + (\nabla \mathbf{u})^T \right] - p\mathbf{I}$

- Cavitation number: $K = \dfrac{p_u - p_d}{p_d - p_c}$

  p_u Upstream pressure

  p_d Downstream pressure

Governing Equations

- Navier-Stokes equations

$$\rho \left(\frac{\partial \mathbf{u}}{\partial t} + \mathbf{u} \cdot \nabla \mathbf{u} \right) = -\nabla p + 2\mu \nabla \cdot \mathbf{D}$$

$$\mathbf{D} = \frac{1}{2} \left[(\nabla \mathbf{u}) + (\nabla \mathbf{u})^T \right]$$

$$\nabla \cdot \mathbf{u} = 0$$

- Finite volume based on QUICK second-order discretization
- Semi-Implicit Pressure Linked Equation (SIMPLE)
- Level-set method for interface tracking and modeling
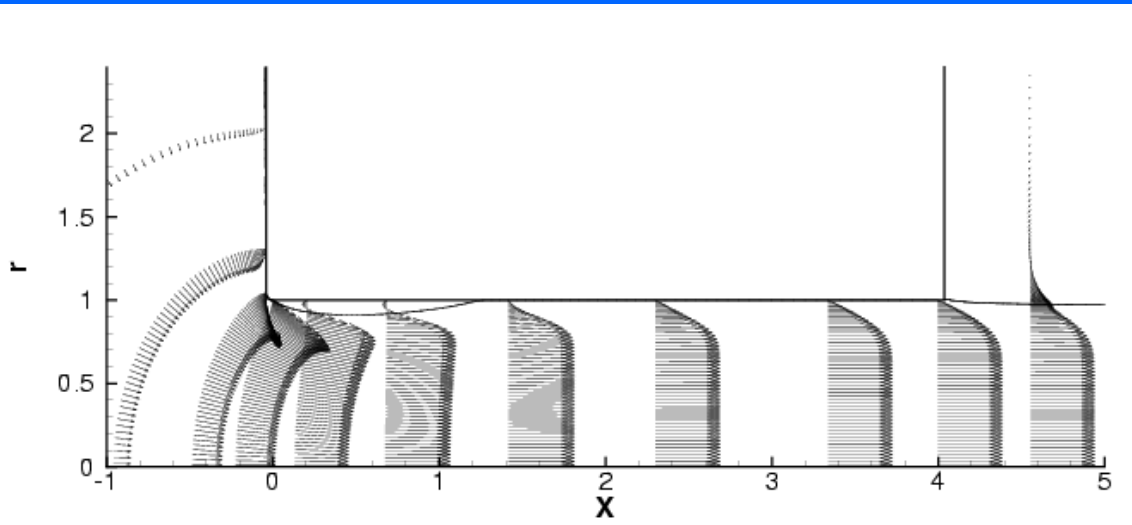
Orifice and jet flow computation

- Computational domain
  - Curved inlet corner
  - Sharp outlet corner
- Boundary conditions
- Grid independency test, 0.5% change when number of grids increased by 50%
- Domain independency test, 0.1% change when domain extended by 50%
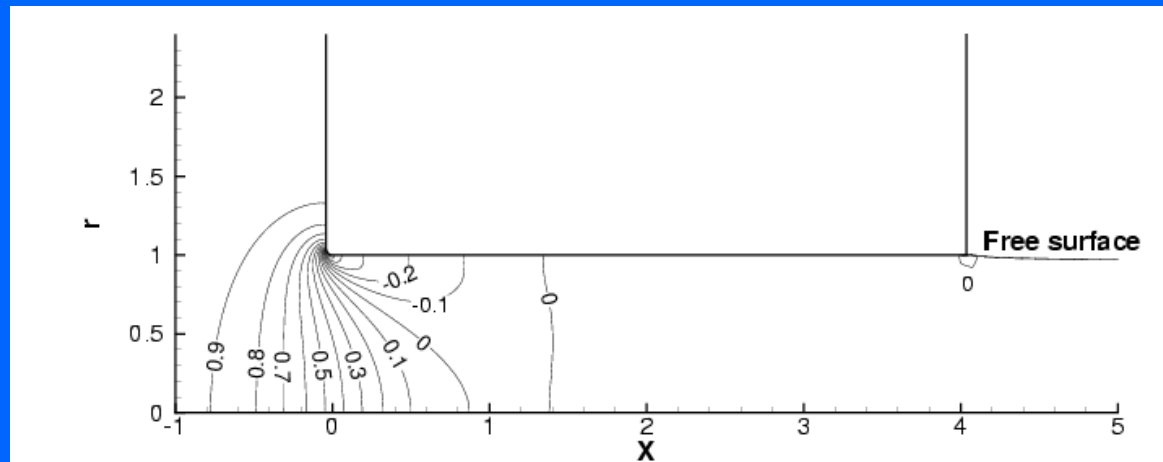

Reservoir

Gas filled chamber
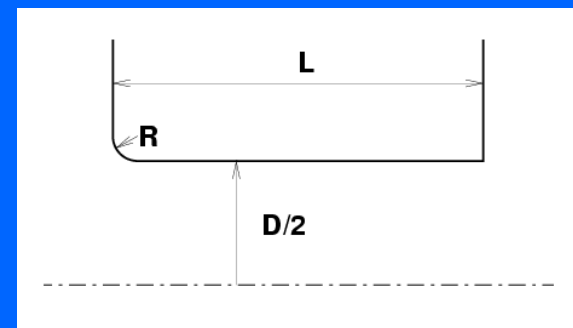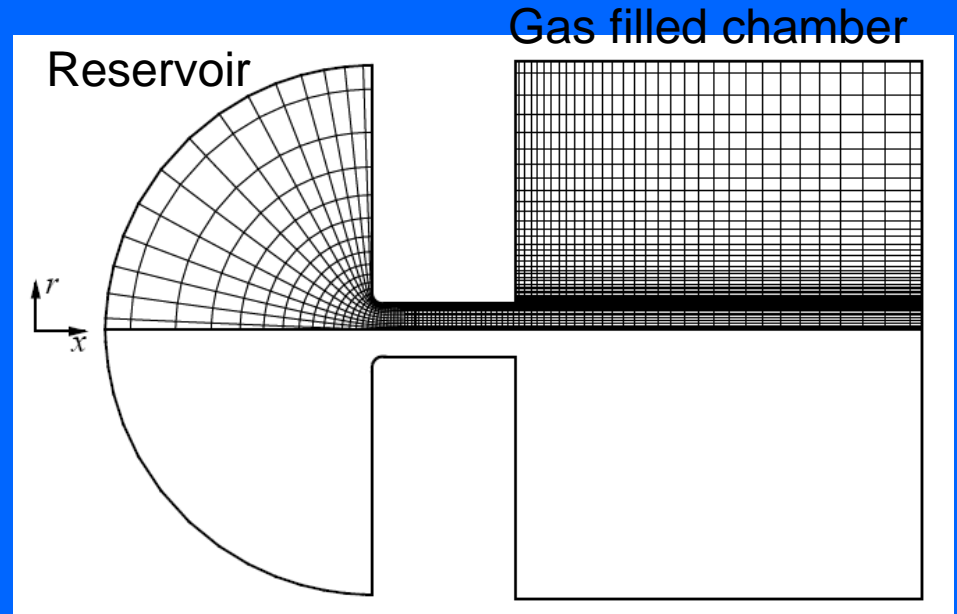
Flow parameters:

$$Re = \frac{\rho_{liq} U D}{\mu_{liq}}, \quad We = \frac{\rho_{liq} U^2 D}{\sigma}, \quad \lambda = \frac{\rho_{liq}}{\rho_{gas}}, \quad \eta = \frac{\mu_{liq}}{\mu_{gas}}$$

Velocity Profile

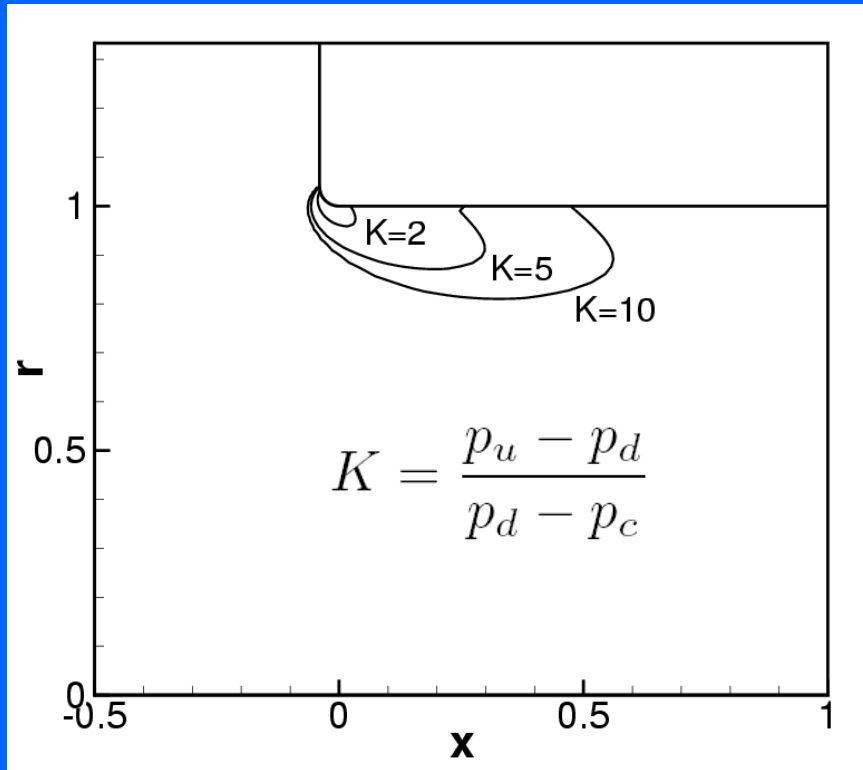

Coefficient of Pressure Contour

Separation occurs with flow around corner.

Consequently, internal flow cross-section reaches a minimum value;
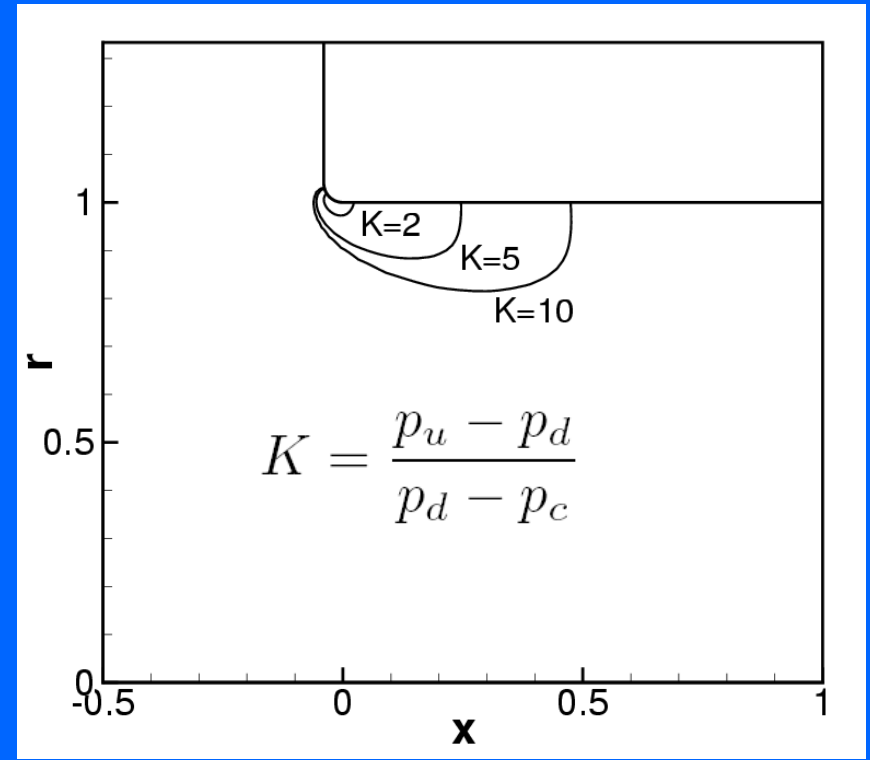
pressure also reaches a minimum value in that region.

In the same region, velocity, rate of normal Strain, and viscous normal stress reach maximum values.
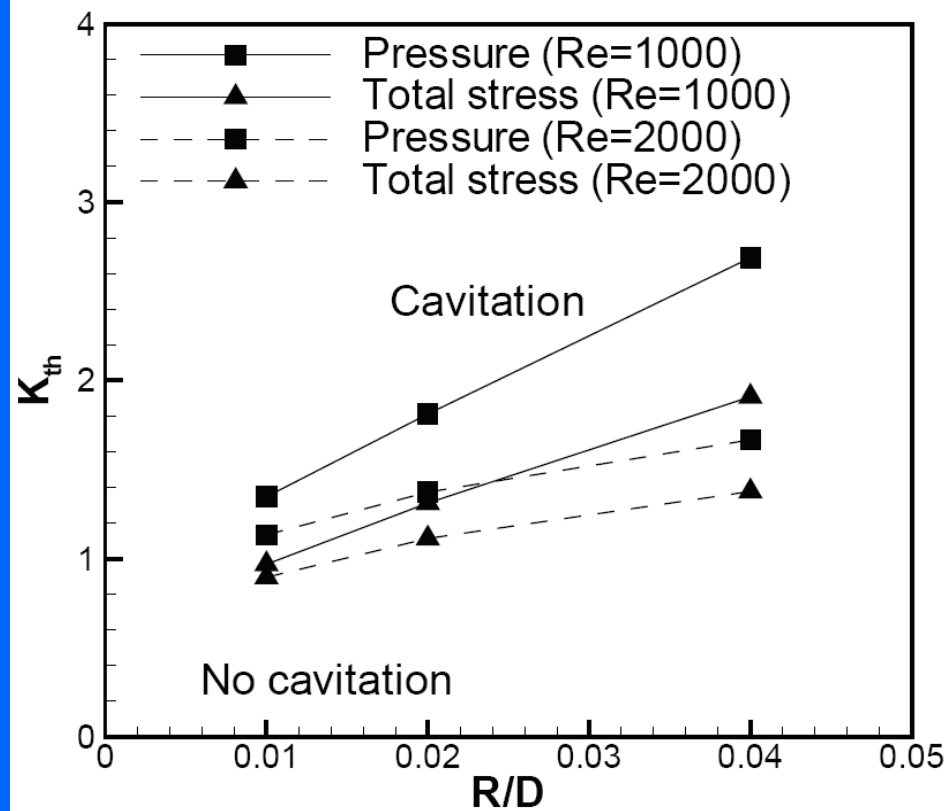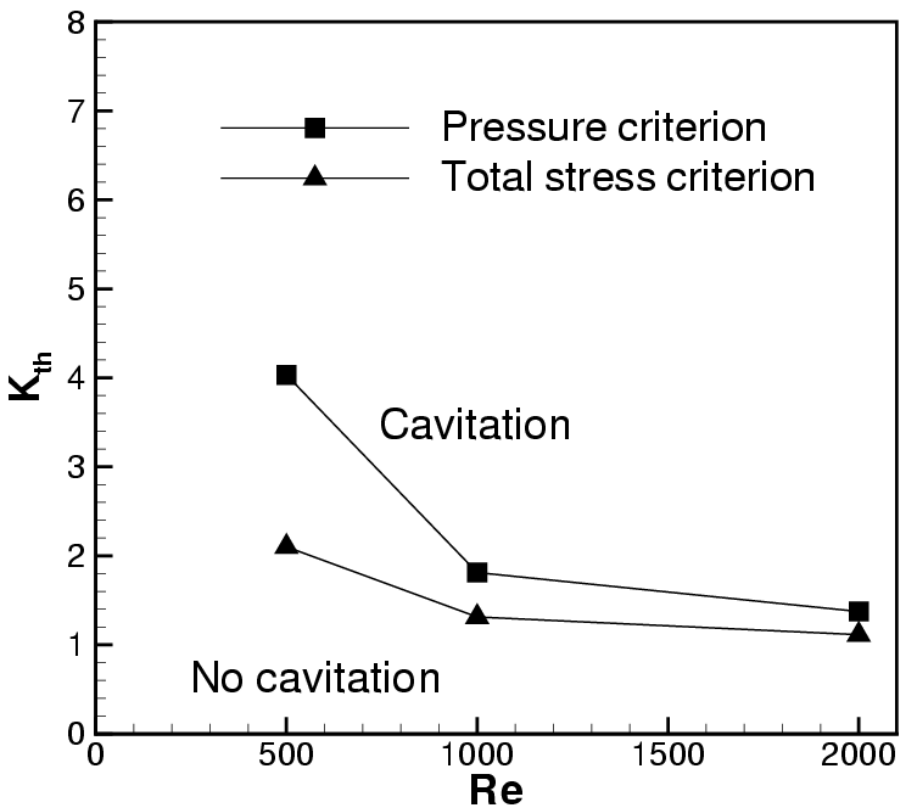
# Total Stress Criterion

Classical Pressure Criterion

For accelerating flow, the rate of strain produces a tensile normal viscous stress. This reduces total normal stress below pressure value. So, cavitation criterion is exceeded by a greater amount and over a larger flow region.

L/D = 2

Cavitation Domain is larger under new total stress criterion and increases with increasing Reynolds number or decreasing radius of curvature at nozzle entrance. The difference between the two domains decreases as reynolds number increases.
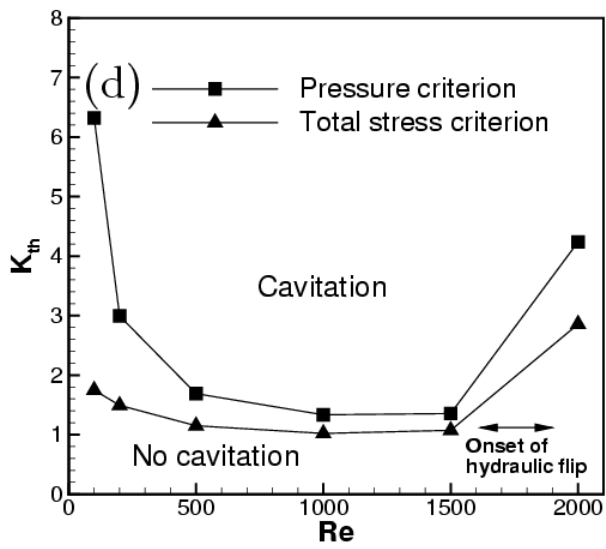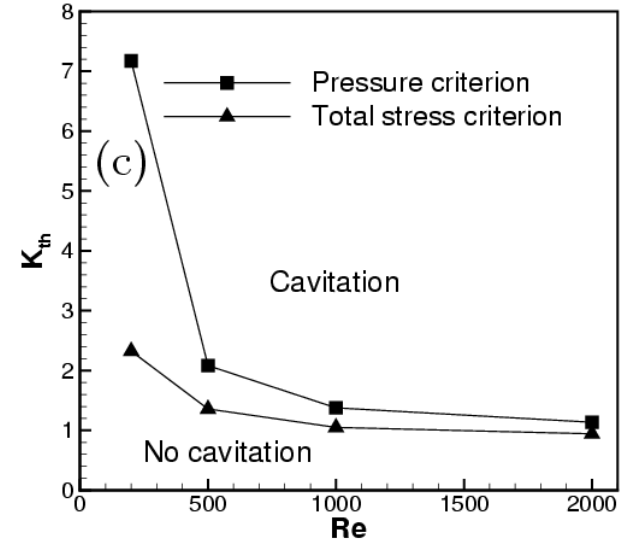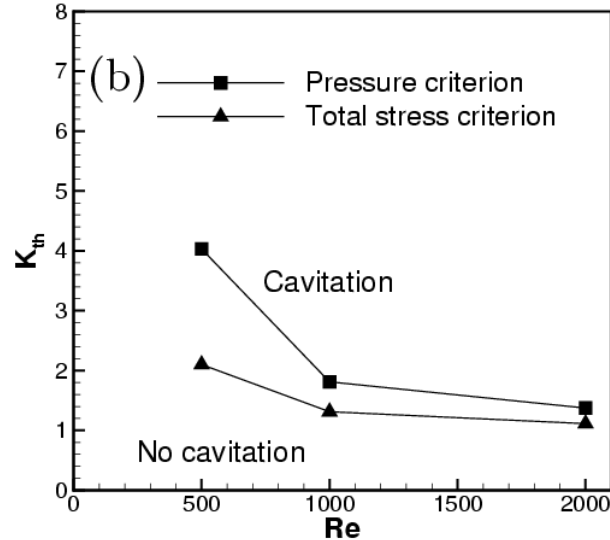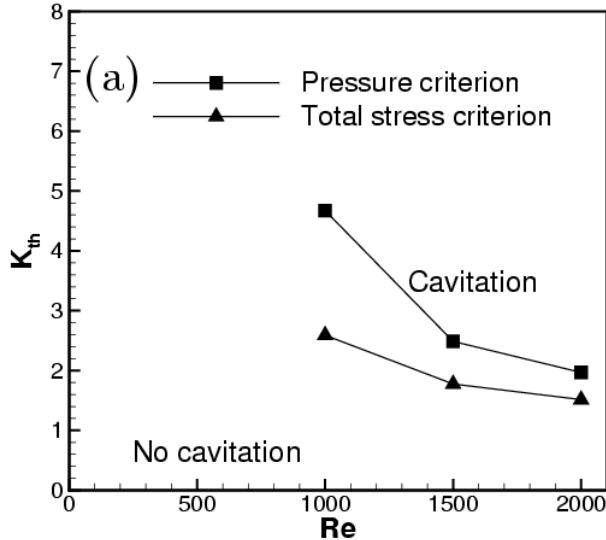
L/D = 5 (a), 2 (b), 1 (c), and 0.5 (d).

To a point, a decrease in orifice L/D increases the acceleration and lowers minimum pressure for the orifice, thereby making cavitation more likely.

For a sufficiently short orifice (low L/D), hydraulic flip occurs. That is, the separated fluid does not re-attach before the orifice exit; gas enters the orifice and pressure becomes more uniform at approximately the ambient pressure, inhibiting cavitation.

# Bubbly Flow Calculations with One-way Coupling

-- axisymmetric Navier-Stokes solution for liquid flow in
     orifice and jet; 3-D bubble and local flow solution.-

-- Each bubble moves with surrounding liquid

-- Varying pressure
   affects bubble
   volume which
   oscillates after
   sudden decrease
   in pressure

-- flow field strain
   affects bubble shape

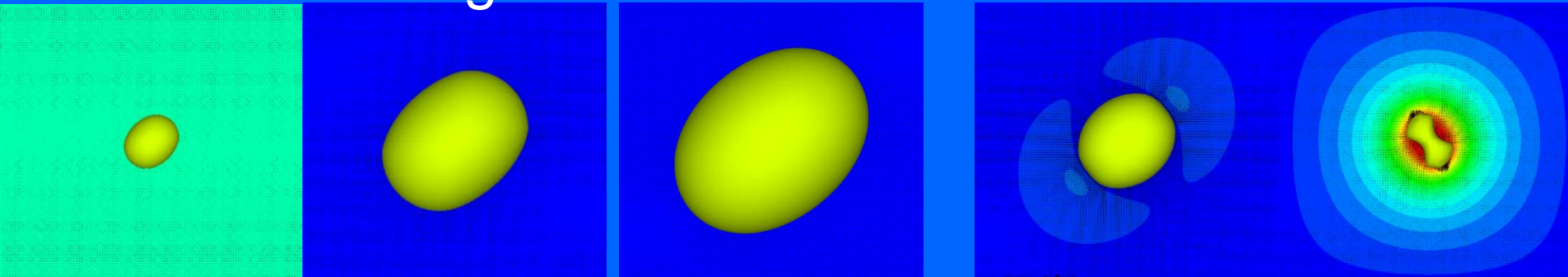-- Bubble dynamics do
   not influence liquid
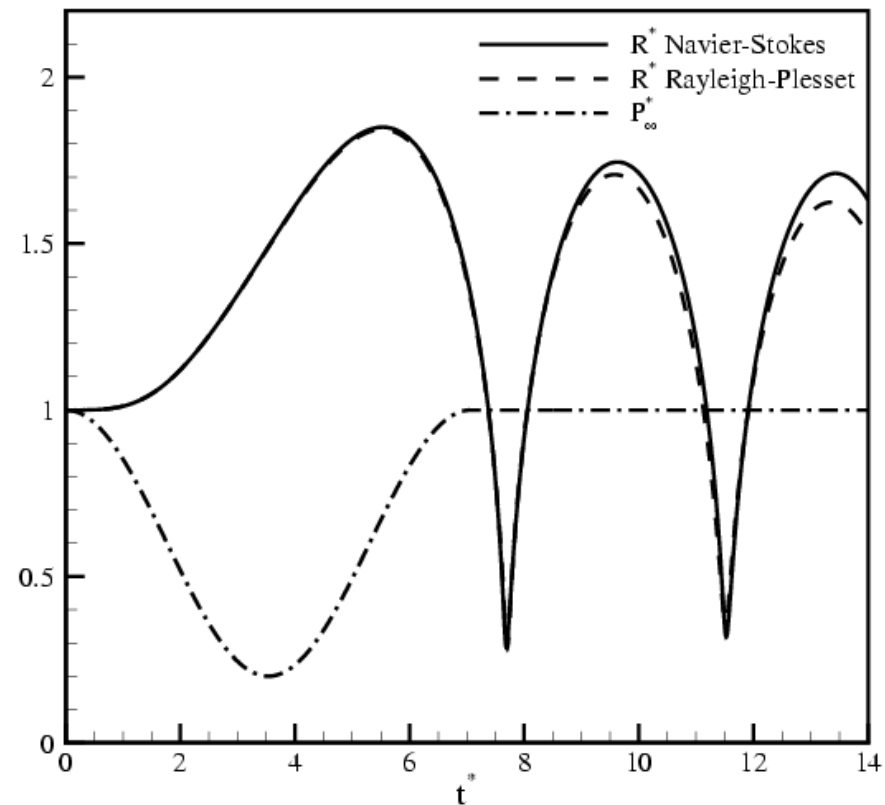
3D N-S calculation for bubble and surrounding liquid
-- Strain causes antisymmetric elongation of bubble.
-- High pressure regions form leading to bubble collapse.
-- Barotropic vorticity formed at density discontinuity.
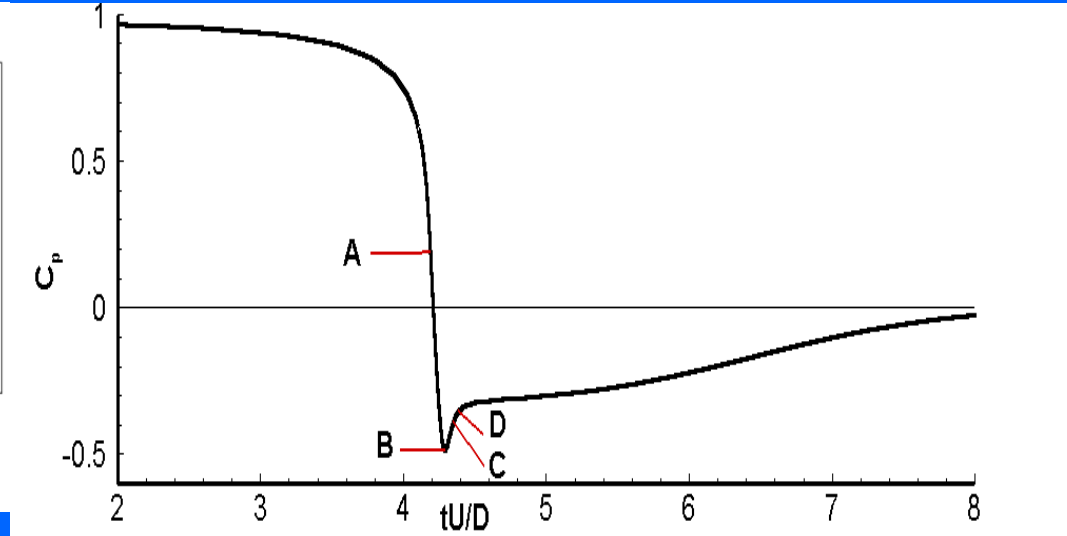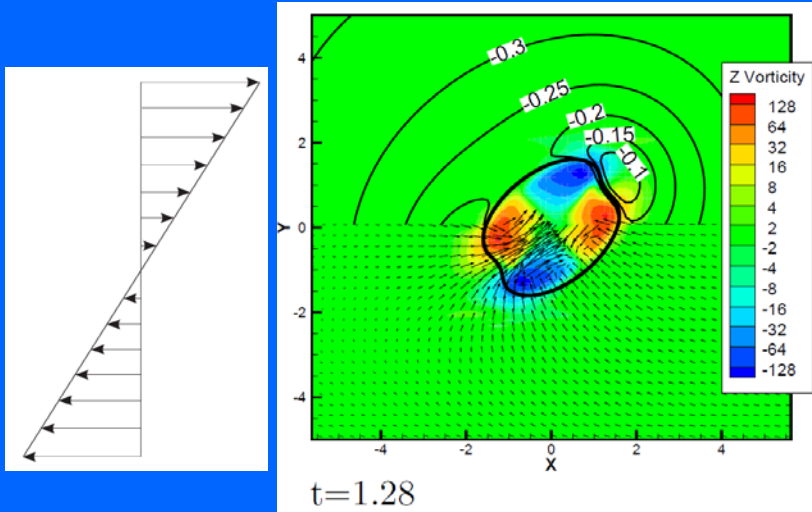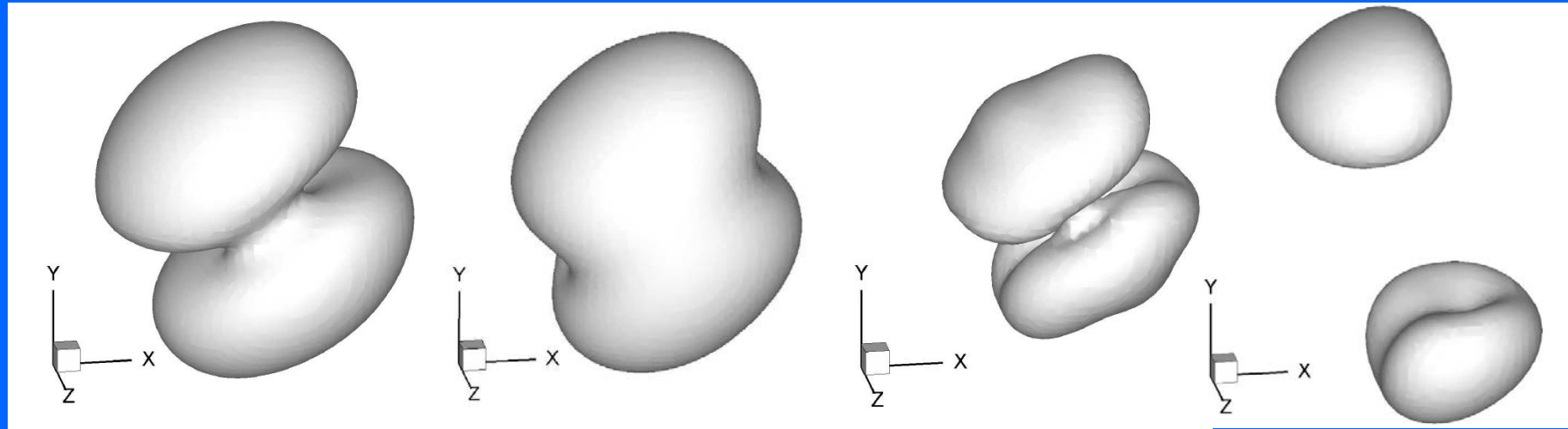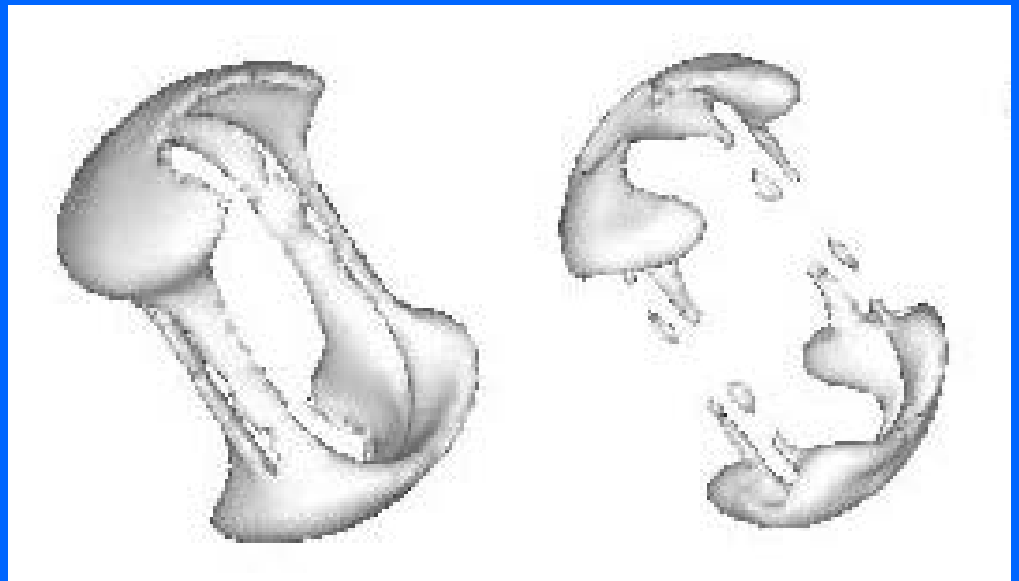

Period of bubble growth and elongation

Period of bubble collapse

Shape of the bubbles after rebound. From left to right: Case 1, Re=1.0, We=0.1; Case 2, Re=0.5, We=0.1; Case 3, Re=1.0, We=∞; Case 4, Re=1.242, We=0.0298.

In some cases with greater pressure variation, holes were formed upon collapse; threads developed connecting two masses and then broke.

Post-processing of far-field around bubble using spherical harmonics to describe disturbance due to bubble dynamics
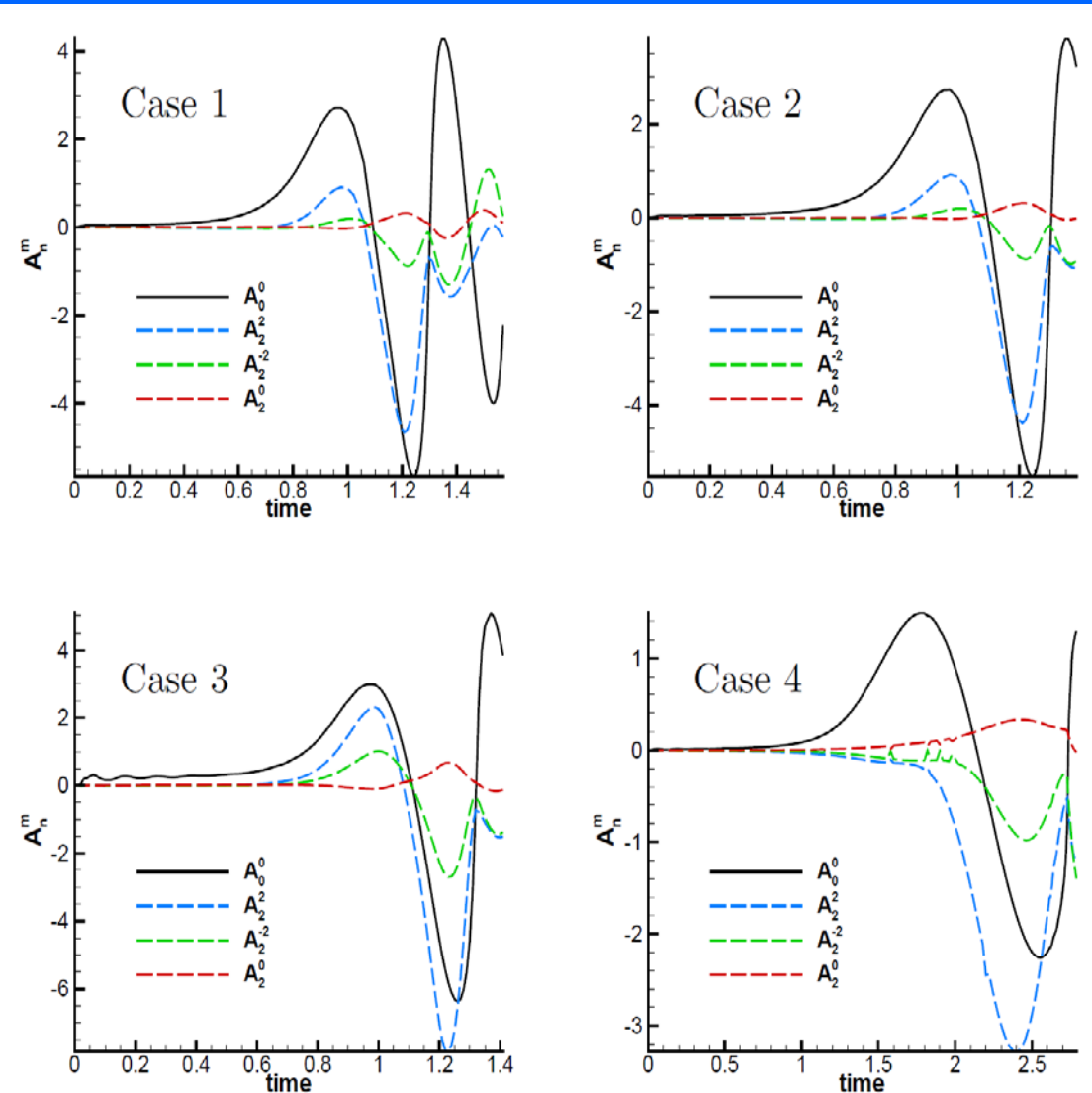
Zero and second-order harmonics in the velocity field. Solid lines represent the monopole and dashed lines represent quadrupoles. No dipoles. Higher order poles are weak.

Monoples drop in strength most slowly with distance from bubble, remain dominant.

Flow with Two-way Coupling

The number of bubbles in the flow were limited in these first calculations.

Only the monopole effect was considered using the Rayleigh-Plesset equation.

$$R\ddot{R} + (3/2)\dot{R}^2 = p_g - p_\infty - (4/\mathrm{Re})\dot{R}/R$$
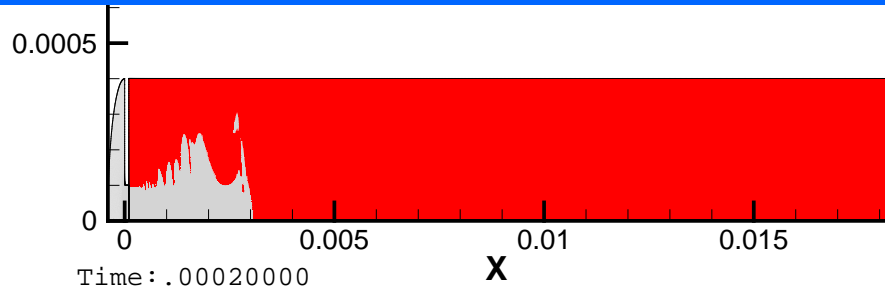$$- (2/We)(1/R)$$

The upper case with bubbles displayed unsteadiness farther upstream compared to lower case without bubbles.

In two-way coupling, bubble volume displaces liquid in contrast to the volume neglect with one-way coupling. Now, the mixture is compressible.
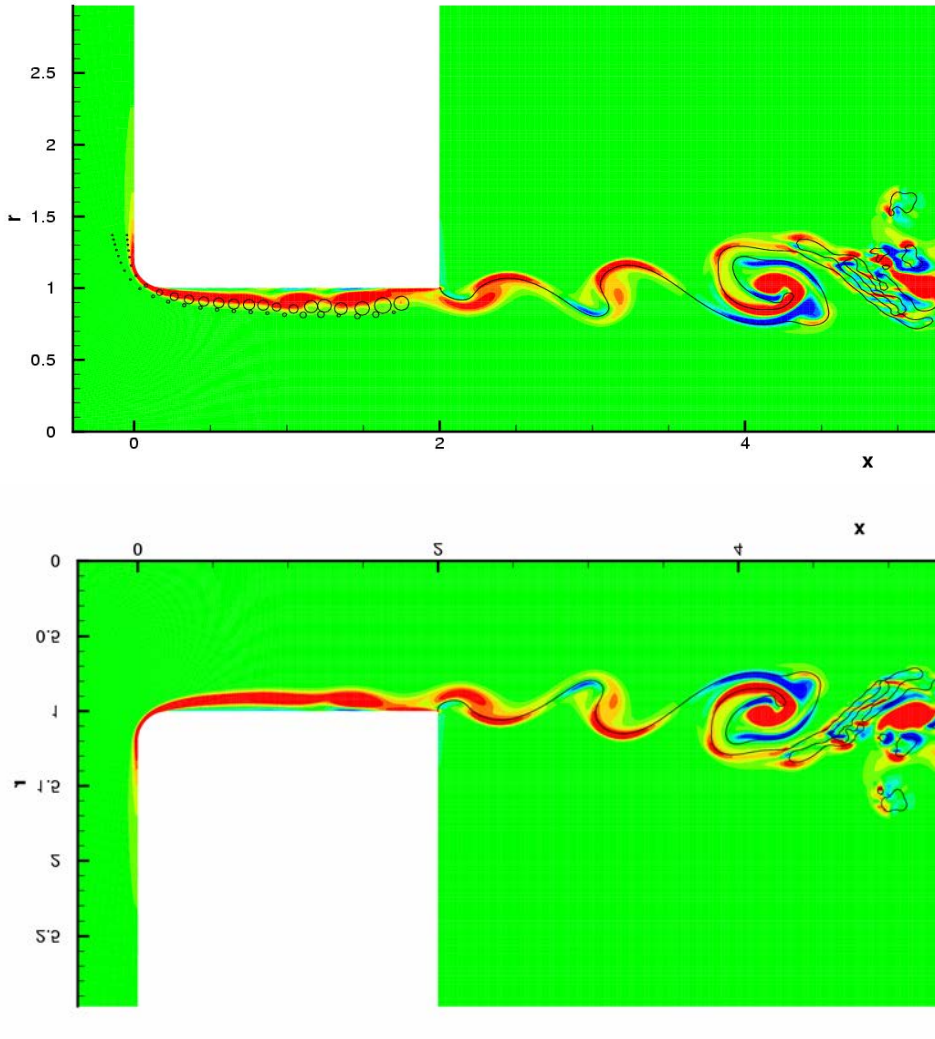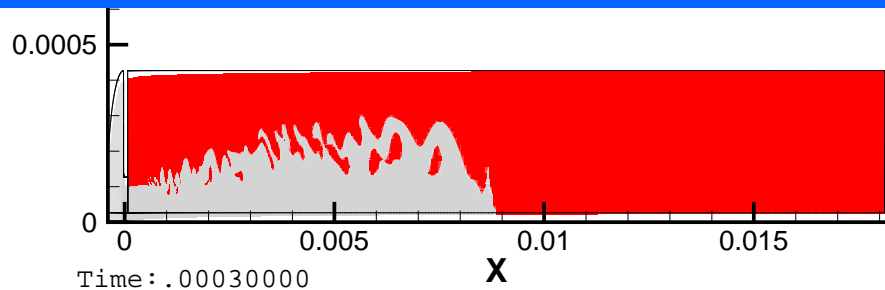
Pulsed Injection of Round Jet Axisymmetric Navier-Stokes with Level-Set

Start-up transient.
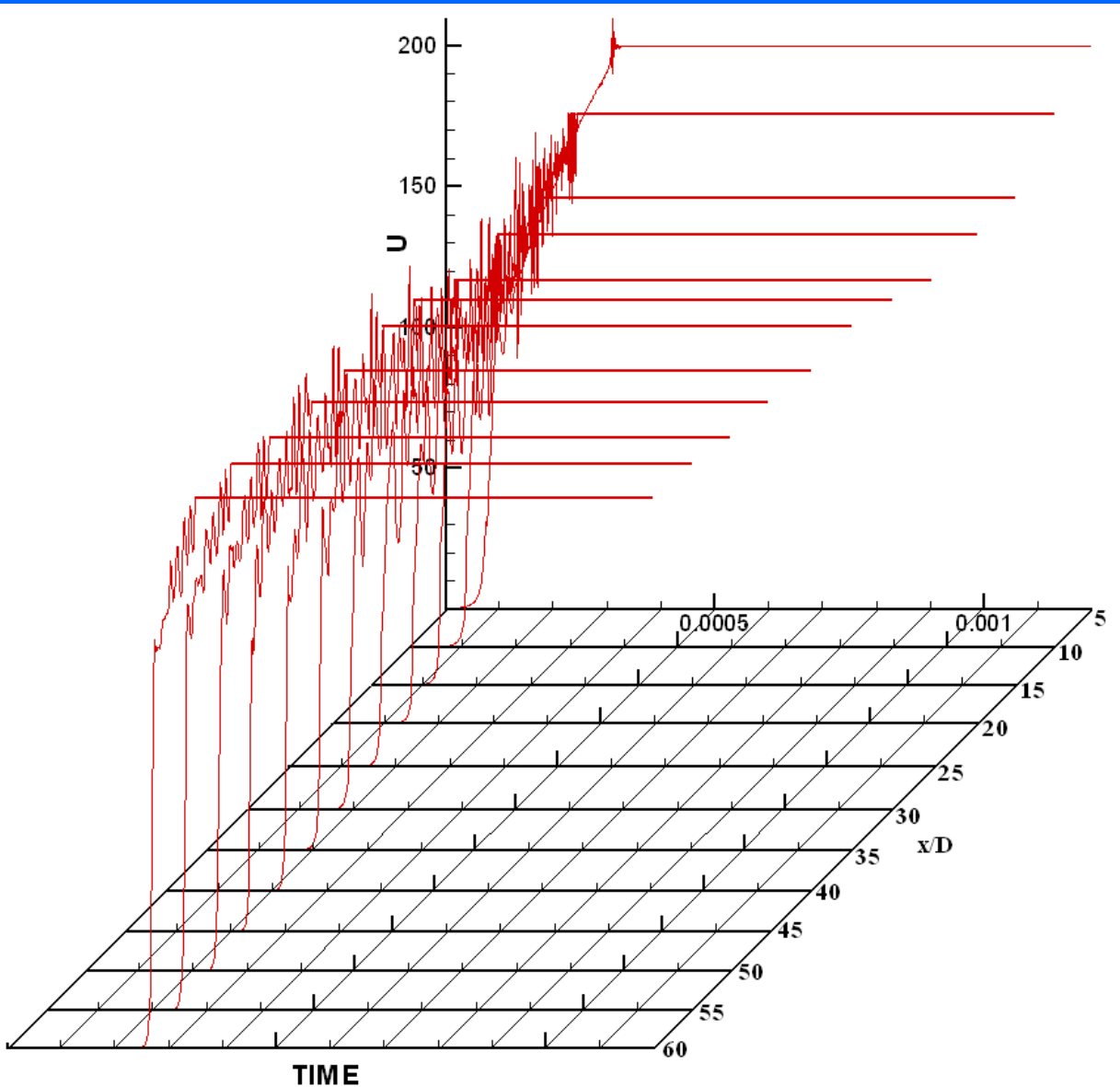0 – 0.2 millisec
Supply pressure rising.

Steady supply pressure.
0.2 – 0.3 millisec
Jet extending.
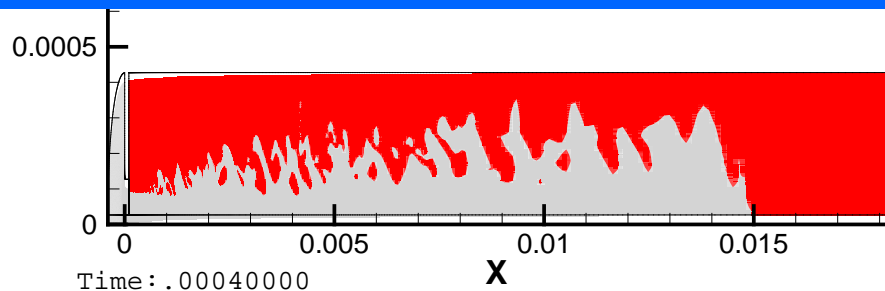
Shut-down transient.
0.3 – 0.4 millisec
Jet still extends.

Jet Centerline Velocity versus Time and Downstream Position

Jet arrival delay increases with downstream distance.

A sharp rise of velocity in time to a plateau value.

The plateau value decreases with downstream distance due to drag.

SUMMARY   REMARKS

- Reduced‑dimension approach is a useful tool and can predict early distortion and breakup length of liquid films.

- Two basic film wave modes, dilational and sinuous, occur.

- Nonlinear effects can significantly modify waveform, breakup length, and coupling between two modes.

- Setting of boundary conditions is delicate; group velocity must be known.

- Film divergence and subsequent thinning in 'conical' flow have significant impact on capillary wave and breakup.

- Effect of gas inertia can be important at high gas density.

- Liquid films can thin in three dimensions forming spots which tear.

SUMMARY   REMARKS continued

- Normal-Stress criterion indicates why and how cavitation can occur at high pressures.

- Orifice design affects cavitation.

- Bubbles grow, distort, and collapse under the varying pressure and flow rate of strain in the orifice flow.

- Monopole and quadrupole disturbances result from the bubble dynamics.

- Monopoles dominate in the far-field and are well described by the Rayleigh-Plesset equation.

- These monopoles enhance shear layer instability.

- Startup and shutdown transients introduce new concepts for liquid jets, e.g., local accelerations, finite jet lengths.

THANK YOU.